#41

QUARTERLY Newsletter

Mercator Ocean
Ocean Forecasters

SPECIAL ISSUE with Coriolis

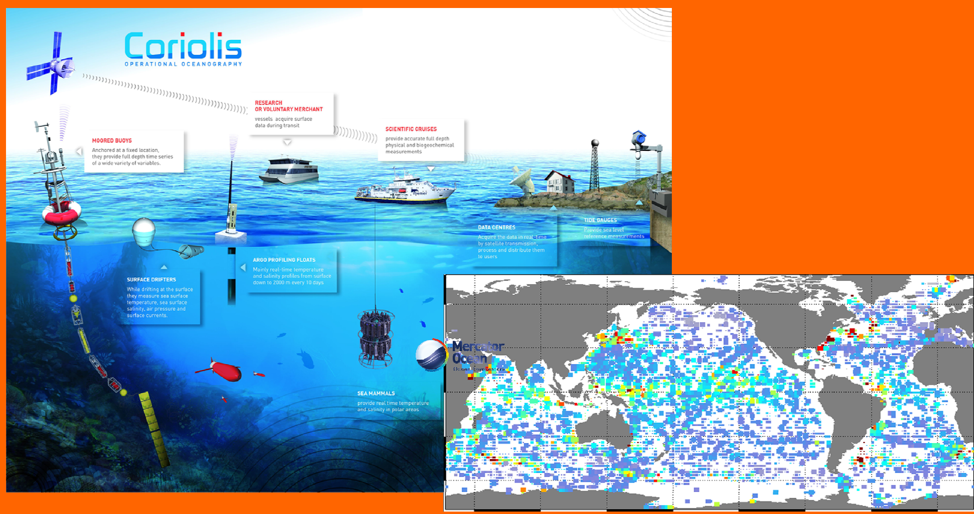

The Coriolis Data Center in Brest is gathering Global Ocean In Situ Observations (top panel), which are then used by the Mercator Ocean Forecasting Center in Toulouse in order to estimate the quality of its numerical simulations outputs (bottom panel, presenting the Mercator Ocean RMS misfit for the 0-500m temperature global ocean in Jan-Feb-Mar 2011 with a color scale from 0 to 2 deg Celcius). Credits: Coriolis& Mercator Océan

Editorial – April 2011 – Special Issue jointly coordinated by *Mercator Ocean* and *Coriolis* focusing on Ocean Observations

Greetings all,

Once a year in April, and for the second time after the April 2010 issue, the Mercator Ocean Forecasting Center in Toulouse and the Coriolis Infrastructure in Brest publish a common newsletter. Some papers are dedicated to observations only, when others display collaborations between the 2 aspects: Observations and Modelling/Data assimilation.

The two first papers introducing this issue are presenting the data requirement for the GMES Marine Core Service (Le Traon and Pouliquen) and the Eurosites Open Ocean Observatory Network (Larkin et al.).

Then, Doxaran et al. are writing about the Provpanache project which uses of ProvBio floats to study the dynamics of suspended particles in river plumes. Two papers are then dealing with eXpendable BathyThermograph (XBT) observations: Hamon et al. start with “Empirical correction of XBT fall rate” and shows that maximum heat content in the top 700 meters found in earlier studies can be explained by now identified XBT biases. XBT are also used by Maes et al. who look at the geostrophic component of oceanic jets entering in the eastern Coral Seas. Next, Brion et al. are using complementary in situ data among which Thermosalinographs (TSG) for the calibration and validation of SMOS.

The two last papers of the present issue are displaying the collaboration between the Ocean Observations and Ocean Modelling communities: Juza et al. are using a numerical model in order to determine how the Argo array could be extended to better monitor the Global Ocean heat content variability. Drevillon et al. are then presenting the Mercator Ocean quaterly validation bulletin “Quo Va Dis?” which is using the Coriolis data in order to draw the picture of the quality of the Mercator Ocean products.

We will meet again next year in April 2012 for a new jointly coordinated Newsletter between Mercator Ocean and Coriolis. Regarding next July 2011 Newsletter coordinated by Mercator Ocean only, it will display papers about the latest space missions and their use for oceanography and research.

We wish you a pleasant reading,

Laurence Crosnier and Sylvie Pouliquen, Editors.

Contents

In-situ data requirements for the GMES Marine Core Service - Report of a workshop organized by the European Environment Agency

By Pierre-Yves Le Traon[1] and Sylvie Pouliquen[1]

[1] *Ifremer/BREST, Plouzané, France*

Context

The European Environment Agency (EEA) has been tasked by the European Commission to provide in-situ data coordination for GMES (GISC project, see http://gisc.ew.eea.europa.eu/). The main objective of this coordination is to secure through policy process the long term provision of in-situ data required for the GMES services. As part of these activities, a workshop was organized by the EEA on June 1st and 2nd 2010. The workshop objectives were to review the main in-situ data requirements from the GMES Marine Core Service (MCS), to provide an overview of the existing global and regional observing systems relevant to the GMES MCS and to identify the main gaps. The workshop involved about 20 invited participants from EuroGOOS and its ROOSes, MyOcean and representatives from the main in-situ infrastructure components in Europe. This process and approach was supported by EuroGOOS who encouraged its members to provide inputs.

Prior to the workshop, a series of position papers were prepared by the participants. Position papers describe European contributions to the global and regional (EuroGOOS) observing systems as well as to specific transverse networks: Euro-Argo, EuroSITES, FerryBoxes, Gliders, Continuous Plankton Recorder (CPR) and E-SURFMAR. MyOcean and its requirements for in-situ data were also summarized as well as the status and perspectives of the MyOcean in-situ Thematic Assembly Center (TAC). These position papers were revised after the workshop and are included in the workshop report (Le Traon and Pouliquen, 2010). The report provides an estimation of costs of the ocean observing system. It identifies the main gaps and gives a first list of priorities and recommendations. These are summarized in the next sections.

Costs of the ocean observing system required by the GMES MCS

A first estimation of the cost of the global and regional in-situ observing systems that are used and needed by the GMES MCS was derived. These costs do not cover all elements of the observing systems (e.g. repeat hydrography) and do not include ship time costs. The consolidated costs of the in-situ observing system for a given EuroGOOS region range from 5 to 15 Meuros/year with a total cost for all EuroGOOS regions of about 40 Meuros/year. The analyses carried out by EuroGOOS teams suggest that an additional funding of 10 to 15 Meuros/year is required to fulfill GMES MCS needs. Costs for the transverse networks of the global ocean observing system are easier to derive, in particular, for well defined components such as Euro-Argo, EuroSITES and CPR. The cost is estimated to about 25 Meuros/year with a future requirement of about 40 Meuros/year. Taking into account that some of the costs of the transverse networks are also included in the cost estimations for the regional seas, the overall costs for the global and regional observing systems required by the GMES MCS are estimated to be about 50 to 60 Meuros with a future requirement of 70 to 80 Meuros.

Main gaps

The workshop identified three types of gaps: organization, sustainability and long term funding and lack of key observations and/or inadequate space/time sampling.

One of the key main gaps in marine observations in Europe is the lack of sustained funding. There is an acute need to secure longer term agreements between member states and the EU to consolidate observing systems and agree on common open (unrestricted) data policies. Co-funding mechanisms (EU and member states) need be set up for the pan-European components of the in-situ observing systems to address common issues as well as new technological developments.

There is a need to evolve European marine coordination and governance towards a more sustained entity with structured European and national relationships. European links with international coordination bodies should be formally established, such as the European contribution to the international JCOMM structure. Sustained coordination of the different transverse observing networks should also be set up.

There is a lack of key observations and there are major gaps in the space/time sampling of the global ocean and regional seas. More observations are needed. There is a need, in particular, to improve the European contribution to Argo (improved sampling) and develop biogeochemical measurements through FerryBoxes, moorings, gliders and evolution of Argo (Bio-Argo). Effort should be made to ensure that measurements from all European research vessels are distributed in near real time (at least for the physical variables and from some of the main biogeochemical data sets). An R&D project on HF radars to design and coordinate an array of HF radars in Europe would also be very valuable.

Main priorities

The main requirements and priorities for the MCS are already well known. In-situ data (that are assimilated in real time in MCS models and provide strong constraints on the MCS model products) should be given the highest priority. Argo clearly falls in this category together with subsurface data from the tropical mooring arrays. One should then consider observation systems that provide important data sets for near real time validation or verification. This includes deep sea moorings and moored buoys, FerryBoxes, the global drifter array, gliders and HF radars. Priorities should also take into account the maturity and feasibility (Is the technology ready and mature? Is there an organization in place for the long term implementation?).

Preliminary propositions for European short-term or mid-term funding

If a direct EU funding is set up through GMES as planned, it should be used to co-fund transnational (pan-European) systems for the most important priorities. The following list provides a series of preliminary propositions that were discussed during the workshop:

- Short-term (possibly from 2011): Euro-Argo, EuroSITES, support for new or improvement of Ferrybox transnational lines, MCS in-situ TAC
- Mid-term (possibly from 2013) : same as above, contribution to E-Surfmar (drifters and subsurface capability on selected moored buoys), support to pan-European glider lines

Conclusion

The outcome of the workshop is a report that will feed into the EEA GISC project deliverables as well as provide the background for communication with GMES actors at an EU level. A meeting focusing on sustainability is foreseen later in 2011.

The EuroSITES open ocean observatory network: a key ocean infrastructure and in situ data provider

By Kate Larkin[1], Richard Lampitt[1], Maureen Pagnani[1]

EuroSITES co-authors: Sue Hartman[1], Athanasois Gkritzalis[1], Jon Campbell[1], Corinne Pebody[1], Henry Ruhl[1], David Billett[1], Veit Hühnerbach[1], Doug Masson[1], Svein Østerhus[2], Kostas Nittis[3], Vasilis Lykousis[3], George Petihakis[3], Vanessa Cardin[4], Manuel Bensi[4], Fabio Brunetti[4], Roberto Bozzano[5], Sara Pensieri[5], Doug Wallace[6], Johannes Karstensen[6], Christian Berndt[6], Imants Priede[7], Anne Holford[7], Tomasz Niedzielski[7], Lee Hastie[7], Alan Jamieson[7], Laurent Coppola[8], Christian Tamburini[8], Dominique Lefèvre[8], Anne Robert[8], Sylvie Pouliquen[9], Thierry Carval[9], Sylvain Ghiron[10], Octavio Llinás-González[11], Andrés Cianca[11], Oscar Melicio[12], Carlos Santos[12], Anibal Medina[12], Pericles Silva[12], Ivanice Monteiro[12], Melchor González-Dávila[13], Magdalena Santana-Casiano[13]

EuroSITES is a Consortium of 13 partner institutes:

[1]NOC; [2]UiB; [3]HCMR; [4]OGS; [5]CNR-ISSIA; [6]IFM-GEOMAR; [7]UNIABN; [8]CNRS; [9]SOPAB-Oceanopolis; [10]IFREMER; [11]ICCM; [12]INDP; [13]ULPGC

The EuroSITES network

EuroSITES is a 3 year (2008-2011) EU FP7 Collaborative Project coordinated by NOC, Southampton which is enhancing the way the European community observes and monitors the ocean interior, seafloor and sub-seafloor. The EuroSITES network currently supports 9 core open ocean time-series across Europe and focuses on integrating and enhancing the open ocean (full-depth) capacity of multidisciplinary in situ atmospheric and ocean measurements. Each observatory provides high quality datasets of climatically and ecologically relevant variables at key locations strategically chosen for studying ocean processes and phenomena. A component of the international OceanSITES network, the EuroSITES observatories have been integrated to form a lasting network of open ocean reference stations and to take Europe's capability in ocean observation beyond the current state-of-the-art. The network has also funded science missions to enhance the observing capability in multidisciplinary ocean variables and to support the research and development and testing of emerging ocean sensor technology at key locations around Europe (www.eurosites.info). The guiding philosophy for EuroSITES/OceanSITES datasets is for full and open access to data in as short a time as possible, aligning with the GEOSS Data Sharing Principles. As a result, the EuroSITES project has enhanced the telemetry capability of open ocean in situ multidisciplinary variables.

The long-term multi-disciplinary ocean time-series data produced by EuroSITES observatories are currently used by a wide range of stakeholders to produce services and products for society. EuroSITES is a key in situ data provider to the marine component of GMES through MyOcean. This includes daily uploads of physical datasets to MyOcean through the in situ TAC and to the WMO/GTS as SHIP, TESAC and, in future, BUFR bulletins. EuroSITES is also a key stakeholder in the GISC (GMES in situ coordination project) led by the European Environment Agency and the EuroSITES open ocean observatories are now considered as a vital in situ platform for producing key ocean and environmental data for the GMES Marine Core Service (through MyOcean) and as a contribution to the Group on Earth Observation (GEO).

This article summarises the progress towards integration and enhancement of in situ open ocean fixed-point observation made since 2008 and the current data flow. In addition, we outline the future vision of the network for operational data provision for societal products and services.

Figure 1: Location map for the EuroSITES network. The 9 existing observatories are marked in blue dots. Associated science mission sites are marked in green dots. All 9 core observatories are OceanSITES time-series and others e.g. ANTARES and Posiedon-Pylos are also OceanSITES candidate sites. For more information visit www.eurosites.info for details of variables measured, infrastructure used, time-series length, resolution and near real-time capabilities.

From research to pre-operational in situ ocean observation

Geographically, the EuroSITES observatories are located around Europe in the Norwegian and Mediterranean Seas and the North Atlantic Ocean (see map, Figure 1). The sites were originally established as research driven fixed time-series sites located in climate-sensitive regions (e.g. deep water formation, inflow and key carbon sink regions) or as meteorological and mainly near-surface physical monitoring programmes. Some sites have a long history. For example, Ocean Weather Ship Station (OWS) Mike in the Norwegian Sea (66ºN, 02ºE) is Europe's longest running (since 1948) time-series site. This site has seen a huge shift in the infrastructure used, trialing a sub-surface mooring for the first time as part of the EuroSITES programme. The newest observatory, TENATSO off Cape Verde has <5 years time-series but is now a key site together with three longer-term established time-series in the North Atlantic. All of the 9 core EuroSITES observatories are registered OceanSITES locations, and the EuroSITES network is therefore considered as the European contribution to the OceanSITES international network of deep-water reference stations which includes the HOT (Hawaii Ocean Time Series) and BATS (Bermuda Atlantic time-series study). EuroSITES is also a component of the Global Ocean Observing System (GOOS) and through this initiative EuroSITES provides key in situ atmospheric and ocean data to the Group on Earth Observation.

EuroSITES sustained in situ fixed-point observations

Sustained in situ observations are critical in order to understand the complexity of the oceans and tease apart the natural variation from the longer-term climatic trends. Ocean observatories are key in situ infrastructures fixed at locations in the global ocean and are used to measure biological, chemical and physical variables. These complement other in situ platforms including profiling floats (e.g. ARGO), ships and gliders and remote sensing methods e.g. satellites. The EuroSITES observatories offer a platform for full-depth multidisciplinary sampling from surface to >2000m depth to the seafloor. The mooring line and surface buoy with telemetry capability also offers a platform for sensors and samplers with larger payloads or as test-beds for emerging sensor technology that requires a fixed-platform or are currently not miniaturized for lagrangian platforms (see Figure 2).

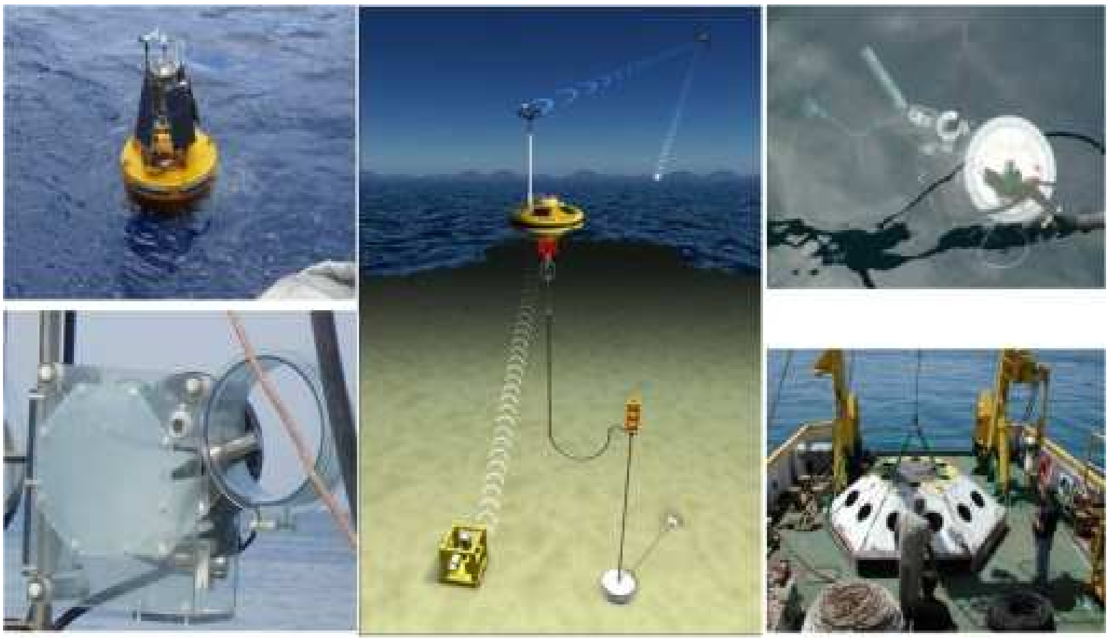

Figure 2: Examples of EuroSITES infrastructures including surface buoys, full-depth moorings, seafloor platforms and novel/emerging sensors (e.g. pH and oxygen consumption).

As a result, the EuroSITES observatories offer some of the highest quality in situ biogeochemical datasets for the open ocean around Europe. These fixed-point in situ data are indispensible as they offer high quality information on the status and health of European seas from real observations. These datasets significantly further knowledge and scientific research, providing vital observations from the surface to the deep-sea with high resolution so that phenomena such as the Northeast Atlantic deep chlorophyll maximum or intermediate waters can be monitored and compared to datasets from other platforms e.g. satellites (e.g. Figure 3). The data are also vital as reference data, providing a fixed data point to compare and merge with spatial information.

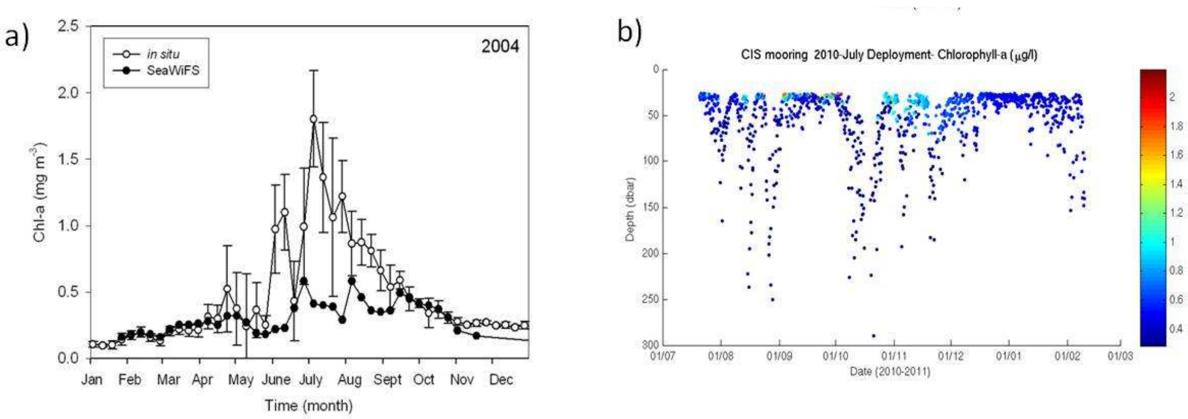

Figure 3: Example biogeochemical (chlorophyll-a) datasets from EuroSITES time-series observatories a) Porcupine Abyssal Plain (PAP) observatory, Northeast Atlantic: in situ quality controlled chlorophyll-a (c.30m depth) data for 2004 plotted against SeaWIFS satellite-derived chlorophyll. The higher magnitude of the in situ data reflects the deep chlorophyll maximum in the Northeast Atlantic which the satellite measurements cannot fully resolve. This highlights the need for in situ measurements to be taken both for vital information but also to validate other observing platforms b) Central Irminger Sea (CIS) observatory: Raw in situ chlorophyll-a data from July 2010-February 2011 as plotted on the EuroSITES website (see link: http://www.eurosites.info/cis/data.php)

Essential Climate variables and indicators

Building on previous National and European (e.g. ANIMATE, MERSEA) funding, the EuroSITES network currently uses moorings and other infrastructure to observe, sample and deliver a unique set of climate sensitive atmospheric and oceanographic datasets in a high quality and sustained manner from the open ocean with full resolution of seasonal cycle down to sub-diurnal cycle. Many of these variables are Essential Climate Variables (ECVs) as defined by the Global Climate Observing System (GCOS) (see: http://www.wmo.ch/pages/prog/gcos/) (see Figure 4). EuroSITES platforms also monitor other variables (currently non ECV's) including oxygen, irradiance, pH and particle flux. Many of these variables can also be used to produce further derived datasets and products which are useful both for modeling applications but also for European policy makers as indicators for good environmental status of the European Seas, contributing to the Marine Strategy Framework Directive (MSFD).

Domain	Essential Climate variables (ECVs) as defined by GOOS
Atmospheric ECV	air temperature, precipitation, air pressure, wind speed and direction
	surface radiation budget and water vapour
Oceanic Surface ECV	sea surface temperature, sea-surface salinity, currents, ocean colour
	chl-a from fluorescence), carbon dioxide partial pressure, sea level, sea state
Oceanic Sub-surface ECV	temperature, salinity, currents, nutrients, carbon system,
	phytoplankton (chl-a from flourescence), ocean tracers
	oxygen, irradiance, nitrate, pH and particle flux
Key	Red = ECV measured by the EuroSITES observatory network
	Black = ECV not currently measured by the EuroSITES observatory network
	Blue = Additional variable (non ECV) measured by the EuroSITES observatory network

Figure 4: Essential climate variables (ECV's) as defined by the Global Climate Observing System (GCOS) (see: http://www.wmo.ch/pages/prog/gcos/). ECV's currently measured by the EuroSITES network are marked in red. Other ECV's relevant to EuroSITES moorings are in black. NB. EuroSITES platforms also monitor other variables (currently non ECV's) including oxygen, irradiance, nitrate, pH and particle flux.

EuroSITES observatories are deep (>1000m) and open ocean, but many of the locations are near to or within Exclusive Economic Zones (EEZs) of European counties. EuroSITES datasets can therefore contribute vital in situ observations for analyzing the environmental status of our European seas for instance monitoring the variation and trends in both physical and biogeochemical variables e.g. temperature currents, productivity, biological diversity and food webs. These datasets, , can be used to understand both the open ocean environments and as a vital early warning system for coastal and littoral regions. During the project lifetime, EuroSITES has also enhanced the seafloor and integrated observational capability with seafloor science missions and by linking with other seafloor monitoring initiatives through joint funding and sharing expertise and know-how with networks including ESONET. In the future, it is anticipated that the EuroSITES fixed-point observatories could be used as platforms to monitor a larger suite of variables including passive acoustics, hydrocarbons and pollutants and as a test-bed for trialing emerging technology for biological and biogeochemical sensors including molecular and genetic sensors/samplers to further define how the biological diversity and food webs may be changing as a result of natural variation and man-made impact. The platforms could also develop as key locations for the monitoring of geohazards including tsunami warning systems, fluid flow/pore pressure, seismic, contributing to GMES and GEO – GEOSS.

A boost for open ocean biogeochemistry

Throughout the EuroSITES project lifetime, the suite of variables and the capability for near real-time data delivery has been further enhanced. As a result, many of the EuroSITES datasets are now available in near real-time (e.g. physical variables and biogeochemical including chlorophyll-a, nutrients, pCO2, O2). The current capability for near real-time data delivery by the network is shown in Figure 5. These data can be used for validation and reanalysis applications and can also be assimilated in forecasting models, provide calibration and validation of both models and space-based information; and contribute to analyses from other platforms.

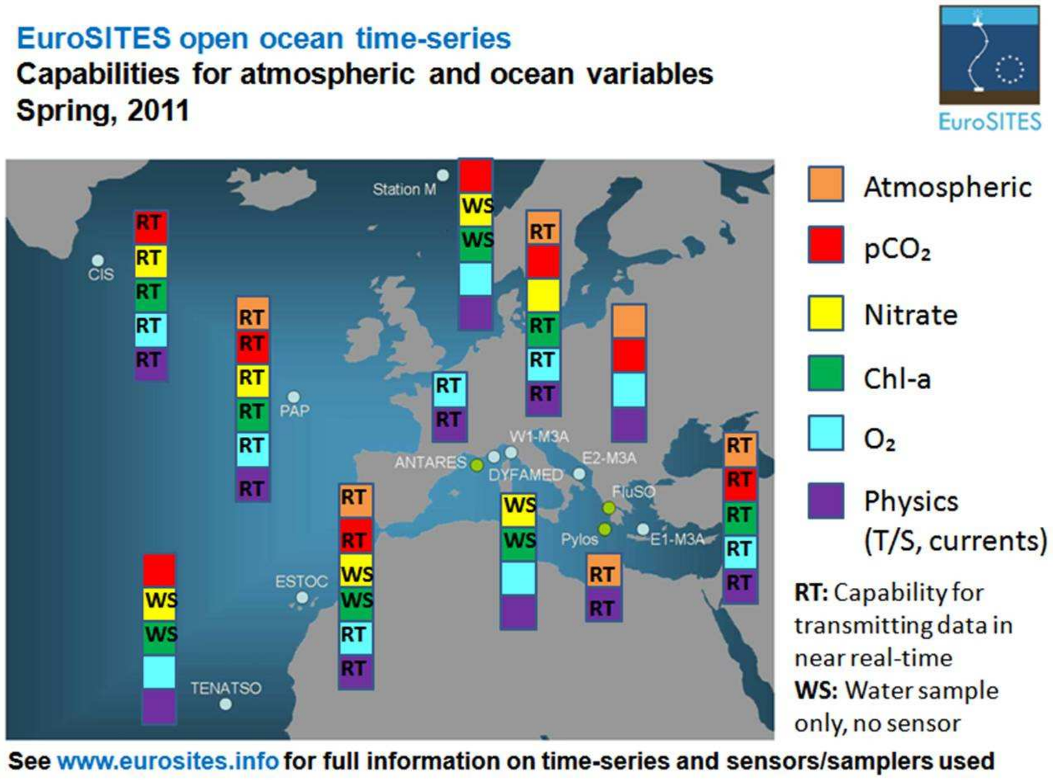

Figure 5: Summary of the EuroSITES network capability (during Spring 2011) for multidisciplinary in situ atmospheric and ocean variables. NB. Variables with the capability for near real-time data delivery are marked as RT. Variables taken by automated sensor in delayed mode only are unmarked. Measurements conducted by regular (e.g. monthly) cruise visits, not an automated sensor are marked as WS. Full details on the current status of each observatory e.g. actual real-time data transmission, sensors and samplers used and the full time-series for each site are available at www.eurosites.info.

EuroSITES: A key stakeholder in GMES Marine Core Service

Because of the unique datasets it produces, EuroSITES is a key data provider of in-situ ocean and atmospheric environmental datasets for GMES through the Marine Core Service. EuroSITES is also considered as a key stakeholder in the GMES in situ coordination (GISC) project which is coordinated by the EEA and financed by the EU's 7th Framework Programme. In June 2010 Kate Larkin (EuroSITES project manager) presented a EuroSITES position paper alongside other key in situ ocean data providers including EuroARGO, FerryBox, Gliders, Continuous Plankton Recorder)(SAHFOS) and the Surface Marine observation programme (E-SURFMAR) at a meeting on 'In situ data requirements for the GMES Marine Core Service'. The aim was to discuss priorities for the global and regional in-situ observing system required by the marine component of the European Initiative GMES (Global Monitoring for Environment and Security). The GISC project is ongoing (January 2010 – December 2012) and in January 2011 EuroSITES coordinators responded to the initial stakeholder consultation process of GMES in situ data requirements and priorities which will produce a comprehensive catalogue of stakeholders.

EuroSITES data management: Open access and near real-time data delivery:

A crucial part of EuroSITES integration has been through data management initiatives. Early in the project all partners endorsed a common data policy of:

- open and full data access in as short a time as feasible
- Delivering data in formats and with sufficient metadata to enable web-based services such as the Sensor Observation Service (SOS) be used to expose and use the data.

As a European component of the international OceanSITES network, EuroSITES has taken a prominent role in developing the OceanSITES data and metadata standards, which EuroSITES uses as its preferred distribution method. EuroSITES data can be viewed online at www.eurosites.info and downloaded as OceanSITES NetCDF files through the OceanSITES Global Data Assembly Centres (GDAC).

The EuroSITES data management team have also been working to increase the near real-time delivery of EuroSITES data to the World Meteorological Organization Global Tele-communication System (WMO/GTS). Currently ocean temperature and salinity datasets from at least three EuroSITES observatories are distributed to the WMO/GTS in near real-time as SHIP, TESAC or in future BUFR bulletins. Meteorological data from the sites are also already delivered as SHIP bulletins. This makes EuroSITES ocean and atmospheric datasets available to a wide audience of potential users as part of the World Weather Watch framework.

All OceanSITES data and metadata are available from two Global Data Assembly Centers, one in Europe (CORIOLIS), one in USA (NDBC). In 2010 the OceanSITES data management teams agreed on the changes required to enable the two GDACs to begin daily synchronization. Since early February 2011 all EuroSITES data files made available to the European GDAC are also made available on the US GDAC. In addition, in cooperation with US-NDBC (National Data Buoy Center), all OceanSITES/EuroSITES data and metadata are now available online as an OPeNDAP resource. The OceanSITES OPeNDAP server is directly serving the content of the files stored on the US GDAC, and a European equivalent is currently planned by CORIOLIS.

Throughout EuroSITES, the network has worked together with ESONET personnel to move towards harmonised data management. One example is the integration of EuroSITES datasets (PAP and Poseidon-Pylos) into the ESONET data portal, achieved by EuroSITES data managers Maureen Pagnani and Thierry Carval working together with ESONET personnel (particularly Robert Huber).

EuroSITES in situ data for Monitoring and Forecasting

The main link and use of EuroSITES data by operational modelling centers is done through the MyOcean In Situ Thematic Assembly Centre (TAC). The in situ EuroSITES datasets are first made available in near real-time on the EuroSITES website (www.eurosites.info). As an integrated pan-European capability, EuroSITES data management led by NOC, Southampton and coordinated with IFREMER then integrates these data into the In situ Tac portal for Monitoring and Forecasting Centres (MFC). Daily delivery of EuroSITES physical datasets is already achieved via both to Global Telecommunication System (GTS) and through MyOcean. The data can then be used both by the global and regional MFCs from MyOcean but also available to EuroGOOS through shared portals. EuroSITES platforms are already being used as reference sites to monitor model behavior and this is set to increase as the availability of EuroSITES data (both physical and biogeochemical) variables in near real-time increases. EuroSITES physical variables e.g. temperature and some EuroSITES/OceanSITES products are already displayed on the MyOcean website as daily deliveries under 'Global Ocean-In-situ Observations'. In addition, more EuroSITES data are available in near real-time (less than one day resolution) than ever before. This has been particularly challenging for biogeochemical data where Quality Control procedures are not all currently automated and manual checking and metadata inclusion are still vital steps to the data flow. In the future, the aim is for EuroSITES observatories to deliver even more data (both physical and biogeochemical) in near real-time to maximize the use of these data in modeling applications, by Monitoring and Forecasting Centres (MFC) including both MyOcean and EuroGOOS.

Mercator-Ocean applications using EuroSITES data

There are ongoing communications and developments between EuroSITES and Mercator-Ocean (Marine Biogeochemistry team) to utilize EuroSITES datasets e.g. chlorophyll, nitrates, CO2 (by order of priority) for validating two global biogeochemical simulations (particularly for the time-period 2002 – 2008). This will extend the work already carried out using data from other OceanSITES observatories BATS (Bermuda Atlantic Time Series) and HOT (Hawaii Ocean time-series study) stations. EuroSITES in situ biogeochemical datasets are being used in reanalysis applications using the model PISCES. This multi-nutrient (ammonium, nitrate, phosphate, silicic acid and iron) and multi-plankton biogeochemical model simulates the biogeochemical cycles of carbon and oxygen and requires in situ datasets for validation. So far, the team at Mercator-Ocean (particularly Coralie Perruche) have run this model globally at a resolution of 1, making global biogeochemical hindcast simulations (1°), forced either with a free physical run at 1/4° or with a physical reanalysis at 1/4°. EuroSITES datasets can provide real observations of some of the 24 prognostic variables (e.g. chlorophyll-a, nutrients, O2) and some diagnostic variables (e.g. sea to air CO2 flux and derived primary production). By the end of 2011, Mercator-Ocean will produce a near real-time simulation whose products (nutrients, O2, chlorophyll-a) will be available on the MyOcean website. The other simulations (and products) can be requested from Mercator. In the future, it is expected that more biogeochemical datasets will be available in near real-time than currently possible. This will increase the use of these datasets in assessing the validity of current and future near real time biogeochemical system.

National modeling applications: From the open ocean to the shelf seas

The use of EuroSITES datasets in modeling applications at a National level is growing. This includes the use of datasets in both global models and for shelf seas models as new scientific questions and drivers are established and the domain of shelf seas models changes. One example is from the Porcupine Abyssal Plain observatory (PAP) in the Northeast Atlantic. With over twenty years of time-series history the PAP site has more than 9 years of high resolution physical and biogeochemical datasets from a fixed-point mooring. The location at 49N, 16.5W already falls within shelf seas models run by the UK Met Office and data from the PAP observatory (particularly chlorophyll, nitrate and CO2) will in the near future be used to validate and constrain both open ocean and shelf seas models. At the moment the work on this system (FOAM-HadOCC, the UK Met Office open ocean physical-biogeochemical model) is not operational and is part of the R&D activities to (i) understand the model's performance and (ii) assessing its skill. In the future, the aim is to take these systems operational, so that products can be delivered to end-users via the MyOcean project. In addition, although it is beyond the scope of EuroSITES to make coastal measurements, there are clearly coastal networks currently integrating the shelf and shallow seas component of the global ocean observing system. As a contribution to EuroGOOS, EuroSITES observatories are linking with coastal initiatives including JERICO and the European Marine Ecosystem Observatory (EMECO).

EuroSITES contribution to GEO

EuroSITES is a registered contributor to the Group on Earth Observations (GEO) particularly for GEO Task AR-09-03c (led by GOOS, IEEE and POGO). EuroSITES data management endorses and implements the GEOSS Data Sharing Principles of free and open access to datasets, metadata and products in near real-time (or with minimum delay for some biogeochemical and delayed mode variables). Further contributions are through Task ST-09-02., data management and societal benefit areas including climate, ecosystems and biodiversity. Biogeochemical datasets are now considered an essential part of the global ocean observing system, allowing the environmental status and condition of marine ecosystems to be monitored. In the near future, it is expected that EuroSITES datasets (raw and quality controlled/derived datasets and outputs) will be registered for the GEO Data Core.

Future development of EuroSITES

There is a societal need to monitor the marine environment with increasing complexity at a global level in near real-time. There is also a need to enhance the capability for near real-time data flow, quality control and metadata for biogeochemical data and to further integrate data from other observing platforms. To achieve this, EuroSITES is supporting research and development to enhance European capability for in situ observation. Science missions include oxygen consumption, pH, tsunami detection, benthic ecosystems, slope stability, fluid flow.

European ocean observatories can also be platforms to trial emerging technology including molecular and genetic approaches for in situ species identification, aerosol detection and in situ mass spectrometry for biogeochemical speciation, bioluminescence and passive acoustics.

As plans develop for the future EuroSITES network, a crucial aspect of the implementation plan will be analyzing any current gaps in the system either geographically or in terms of key variables not currently measured. This discussion to establish a core set of variables and to identify critical regions which are under-sampled or variables which would assist in research, model and societal applications is something under discussion between the observational and modeling communities within EuroSITES and OceanSITES. There are also a few key locations which are already being monitored by projects including ESONET, EMSO and HERMIONE which could also form part of a future EuroSITES network.

Ocean Observing remains a key European challenge

During the time-span of EuroSITES, the network has progressed from a research driven platform to a pre-operational infrastructure with near real-time data transmission and delivery to a wide range of users. Datasets are now being used in near real-time and delayed mode for modeling applications and as indicators of good environmental status for policy outputs reliant on in situ observations to monitor the state of the sea and the characteristics of the marine ecosystem. In the longer-term the full-depth EuroSITES observatories can be considered as a key component of the European Research Infrastructure EMSO, selected by the European Strategy Forum on Research Infrastructures (ESFRI) on its roadmap for European research platforms. As a result of bi-lateral communication and exchanges, the vision of this infrastructure has widened towards a truly integrated ‘European Multidisciplinary Sea Observatory’. In the future, the vision is for integration both across platforms (e.g. linking moorings to profiling floats, gliders, ships) and geographically from the coast to the open ocean and from the local and regional scale to the global scale.

However, despite these efforts and significant progress towards an operational in situ operational network, there is currently no future EU funding committed to maintain the EuroSITES observatory network beyond April 2011. The current FP7 funding for EuroSITES has been the vital 'glue' funding to integrate and coordinate the existing open ocean time-series stations around Europe. Without sustained funding from both National and European sources, the EuroSITES platforms and will cease to be maintained and enhanced. This will ultimately reduce the data flow and resolution of key in situ open ocean variables.

The future GMES marine service is expected to be operational in just three years time, reliant on in situ ocean data from key platforms including the EuroSITES observatories. In some cases National funding has been secured for the short-term future to maintain some of the EuroSITES time-series. However, what is required is a longer-term commitment from both National and European funders to secure the sustained time-series approach to these infrastructures. Significant and ongoing interaction with relevant projects including ESONET, EMSO, HERMIONE, GISC, EMODNET and OOI has been very productive and paving the way towards sustained funding. Without firm commitments, both for the data services and the collection and enhancement of the data collection and observation infrastructure including EuroSITES platforms services and products will have huge gaps in real in situ datasets in the coming years just at the time when we will have the operational capability to maximize the use of these in situ data.

There has never been a greater need or a clearer societal value for in situ open ocean datasets. In 2009 the decadal OceanObs'09 conference stated that 'Observing the oceans is critical to understand, assess, forecast future threats, and to manage and reduce human vulnerability and risk linked to the oceans'. In 2010, the European marine and maritime community stated 'Ocean Observing' as a key European challenge and priority at both the 2nd ESF Marine Board meeting in Brussels and the EurOCEAN 2010 declaration in Ostend (October 2010). EuroSITES is just one of many key existing infrastructures currently moving European capability towards operational provision of in situ data. The momentum and the drive from the community is there and data providers such as EuroSITES are crucial to the development of a European system for operational monitoring and forecasting of the ocean physics, biogeochemistry, and ecosystems, on global and regional scales.

Acknowledgements

The Consortium would like to thank Sylvie Pouliquen for the invitation to contribute an article to this newsletter and to the Mercator-Ocean Marine Biogeochemistry team (in particular Coralie Perruche and Marie Drevillon) for their interest and information about utilisation of EuroSITES datasets in modeling applications. The authors would also like to thank David Ford and Rosa Barciela Ramos from the UK Met Office for providing examples of EuroSITES datasets to be used in shelf-sea models etc.

The EuroSITES project is coordinated by the National Oceanography Centre in Southampton, UK. The coordinator is Richard Lampitt, the project manager is Kate Larkin and the data manager coordinator if Maureen Pagnani.

Useful links

For further information on the EuroSITES project, please visit the project website www.eurosites.info and the international OceanSITES network www.oceansites.org

The EuroSITES data files are freely available as OceanSITES NetCDF files through the OceanSITES GDACs:

- ftp://ftp.ifremer.fr/ifremer/oceansites/DATA
- ftp://data.ndbc.noaa.gov/data/oceansites/DATA

EuroSITES is a key stakeholder (data provider) for GISC (GMES in situ coordination:
http://gisc.ew.eea.europa.eu/documents/public/general-info

Read more about EuroSITES in the 2010 Earthzine article (June 2010): http://www.earthzine.org/2010/06/26/eurosites-open-ocean-observatory-network-monitoring-europe%E2%80%99s-open-ocean/

Use of ProvBio floats to study the dynamics of suspended particles in river plumes: the Provpanache project.

By David Doxaran[1], Hervé Claustre[1], Marcel Babin[1], Thomas Lorthiois[1] and Antoine Poteau[1]

[1]UMR 7093, CNRS-UPMC, Laboratoire d'Océanographie de Villefranche, France

Introduction

Terrigeneous organic carbon transported by rivers originates from land erosion, rainfall and in situ production. River mouths are land-sea interface which favour the development of estuarine environments where particles supplied by rivers are temporally trapped as a result of the residual density circulation and tidal currents. These estuarine environments either develop in the downstream part of rivers (low river discharge) or in the adjacent continental shelf (high river discharge) (e.g., Dagg et al. 2004). There, the fate of suspended particles supplied by rivers first depends on the mixing between the fresh turbid river waters and salted clear coastal waters. This mixing is controlled by bottom morphology and the physical forcing involved: tidal currents, wind and swell, storms, regional circulation. The stratification of density limits the turbulent energy and enhances the aggregation between mineral and biogenic particles (e.g. Eisma et al. 1991, Dagg et al. 2004, Geyer et al. 2004). This usually results in a rapid sinking of particles which reach the bottom floor within several hours (Dagg et al. 2004). By opposition, the transport of the terrigeneous dissolved organic matter is expected to be more conservative as mainly driven by the mixing between fresh and oceanic waters. However this is more complex in reality as interactions between solid and dissolved substances, both terrigeneous and biogenic (e.g., adsorption processes) also occur (Dagg et al. 2004, Geyer et al. 2004). Moreover, physical and chemical conditions within river plumes (high loads of nutrients, increase of solar light penetration and the resulting photochemical degradation of the organic matter) enhance the primary and microbial production.

Due to such complex dynamic processes, it is difficult to track particles exported by rivers in the coastal ocean and to determine the associated fate of the terrestrial organic carbon. The use of ocean color satellite data only allows monitoring the dynamics of suspended particles within the surface layer (0-2 m depth) (Doxaran et al. 2002, 2009), while the transport of particles is clearly three-dimensional. Field measurements are therefore needed to complement satellite observations and provide information concerning the sinking of particles.

On the global scale, the delivery of terrigeneous organic carbon by rivers into the ocean mainly occurs: (i) in tropical regions where are located the major world rivers (e.g., the Amazon in Brazil and Yangtze in China) and (ii) in the Arctic region (e.g., the Mackenzie in Canada and Lena in Russia) (Schlunz and Schneider 2000). Due to the lack of field measurements in these remote regions and because of the complexity of the processes involved, the fluxes of organic carbon delivered by rivers into the ocean are currently poorly documented.

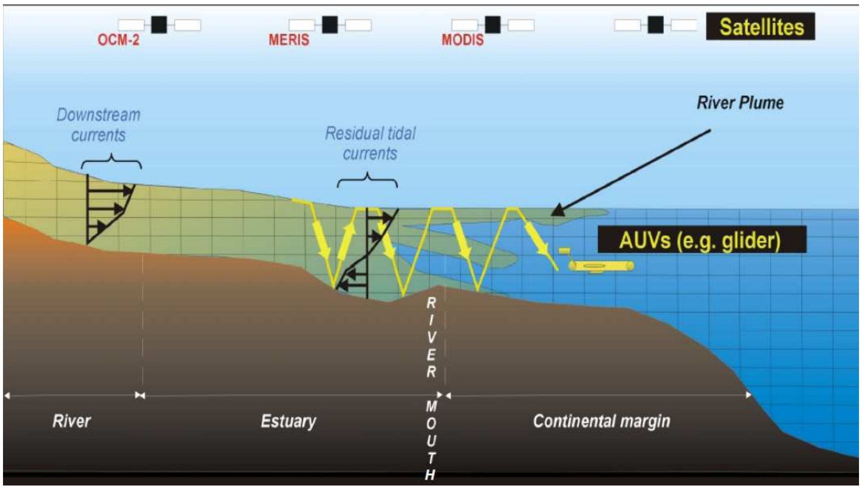

Figure 1: Schematic view of a river plume sampled using ocean color satellite and field data recorded by an autonomous profiling vehicle.

The main objective of the Provpanache project is to use bio-optical profiling floats (ProvBio) to complement satellite observations and provide a three-dimensional view of the dynamics of suspended particles in coastal waters directly influenced by river discharges (Figure 1). While satellite observations provide observations of surface waters potentially every day (depending on cloud cover), bio-optical floats are expected to provide useful information on particulate exchanges and fluxes occurring within the water column.

The first objective is to test the capability of ProvBio floats, originally designed for open ocean waters, in dynamic and shallow coastal waters. The second objective is to combine satellite and ProvBio data to develop an operational autonomous way to monitor the transport and sinking of particles within river plumes, and then better understand the physical processes involved.

Several major rivers in the Arctic and temperate regions are here considered as test sites for deployments of ProvBio floats. Two ProvBio-B floats were used as part the Provpanache project. These floats were developed jointly by IFREMER and the French company KANNAD/NKE, following the scientific directives of the Oceanographic Laboratory of Villefranche (LOV). The design of the ProvBio-B floats were achieved from the Provor-CTS3 float equipped with a CTD sensor and miniaturized optical sensors: a Wetlabs transmissometer (C-Rover), a 3-wavelength Satlantic radiometer (OCR-504) and an "ECO3" Wetlabs sensor, measuring chlorophyll-a fluorescence, colored dissolved organic matter and particle backscattering coefficients.

Deployments of autonomous profiling floats in coastal waters

Considering recent experiments and successes in open ocean waters (Le Reste et al. 2009), the following method was adopted for the deployment of ProvBio floats in coastal waters:

(i) Deployments occurred at the beginning of planned oceanographic campaigns (the floats were programmed to start profiling one day after deployment).

(ii) A systematic cross-calibration was established between the CTD and optical data recorded by the float and those recorded onboard the oceanographic vessel; simultaneously water samples were collected onboard the ship in order to determine the concentrations of the colored water constituents: suspended solids, particulate organic carbon and chlorophyll pigments. The aim was to establish calibration relationships between the optical and biogeochemical measurements.

(iii) During deployments, the ProvBio were profiling daily (one or three profiles a day during daytime) and data were transmitted daily for real-time data processing and display (www.obs-vlfr.fr/OAO/, P.I. A. Poteau (LOV)).

(iv) Match-ups with ocean color satellite data recorded by the MERIS and MODIS-Aqua sensors were systematically identified as part of the GlobColour program (ACRI-ST, www.acri-st.fr/) and displayed on the OAO (Oceanographic Autonomous Observations project of the Laboratoire d'Océanographie de Villefranche) web site.

(v) Oceanographic vessels were available for assistance during deployments and the floats were systematically recovered at the end of the oceanographic campaigns.

In 2009 and 2010, five deployments and recovery were carried out as part of the Provpanache project.

The first deployment occurred in the Beaufort Sea (Canadian Arctic Ocean), directly influenced by the Mackenzie River discharge, during the Malina oceanographic campaign (www.obs-vlfr.fr/Malina/, P.I. M. Babin (LOV)) onboard the ice-breaker Amundsen (Canadian Coast Guard Ship, CCGS). One ProvBio float was deployed on 07/08/2009 at the boundary between the Beaufort Sea and Amundsen Gulf. The objective was to study the seaward export of particles and colored dissolved organic matter delivered by the Mackenzie River. After deployment, the float profiled once a day between water surface and 200 m depth, moving north along 40 km up to the limit with floating sea ice. The float was then ordered to stop profiling and moved south within surface waters up to recovery onboard the ice-breaker Amundsen on the 21/08/2009.

The second and third deployments took place in the Gulf of Lions (western Mediterranean Sea) directly influenced by the Rhone River plume. Deployments and recoveries were conducted from the Antédon II research vessel (CNRS/INSU), as part of the Optic-Rhone oceanographic campaigns (P.I. D. Doxaran (LOV)). The float was initially deployed right in front of the Rhone River mouth (water depth 40 m) on the 10/04/2010. The float was programmed to profile three times a day, successively surfacing at 8h, 12h and 18h local time, and ground during night time in order to limit the offshore drifting. The objective was to study the seaward export of particles supplied by the Rhone River and its impact on the phytoplankton spring bloom. After 40 days of deployment, as a result of an extreme spring flood event, the ProvBio float moved seaward up to the limits of the Rhone River plume. The float was therefore recovered on the 26/05/2010, equipped with cooper film to prevent bio-fouling and redeployed in front of the Rhone River mouth on the 28/05/2010. As the Rhone River discharge significantly decreased after spring flood events, the ProvBio float maintained its position in the Rhone River plume within a 20 km distance from the mouth. The float finally got trapped in fishing nets and was recovered in the harbor of Marseille on the 02/07/2010.

The fourth and fifth deployments took place in the Bay of Biscay (Atlantic Ocean) directly influenced by the Gironde River plume. Deployments and recoveries were conducted from the Côtes de la Manche research vessel (CNRS/INSU), as part of the CAROLS oceanographic campaigns (P.I. G. Reverdin (LOCEAN) and L. Marie (Ifremer)). The float was initially deployed in front of the Gironde River mouth, 15 km offshore (water depth 40 m) on the 08/05/2010. The float was programmed to profile three times a day, successively surfacing at 8h, 12h and 18h local time and ground during night time. The objective was to study the dynamics of the Gironde River plume at the end of the spring flood period. Due to tidal currents, the float maintained its position 20 km offshore the mouth during 40 days. When the impact of bio-fouling clearly showed on the optical measurements, the float was recovered on the 02/07/2010, cleaned and protected using cooper films then redeployed the next day (03/07/2010). The float first maintained the same geographical position then on the 10/07/2010 suddenly started to move upstream and entered the

Gironde mouth through the southern pass on the 25/07/2010 where it was finally recovered on the 02/08/2010. This upstream transport (1 km a day on average during 20 days) has resulted from the combined decrease of the river freshwater discharge and predominant flood currents during spring tides.

Spatio-temporal dynamics of suspended particles

Temperature and salinity data recorded in the Beaufort Sea clearly show a constant stratification with fresher and warmer waters within a thin (20 m) surface layer resulting from both the Mackenzie discharge and sea-ice melting (Figure 2). A slightly vanishing deep-chlorophyll maximum is clearly observed at 60 m depth. A thin (0 – 5 m depth) surface layer characterized by high concentrations of suspended solids is identified using as proxies the measured light attenuation and backscattering coefficients, indicating the presence of the Mackenzie river plume (probably in addition to particles originating from melted sea ice). Patches of non-chlorophyllous particles are also located at 100 m and 200m depths (sinking).

Optical measurements carried out in the vicinity of the Rhone River plume clearly show the co-existence of a surface plume and a bottom nepheloid layer both characterized by high loads of suspended solids, while biogenic particles develop 20 km offshore the river mouth to form a deep-chlorophyll maximum (Figure 3).

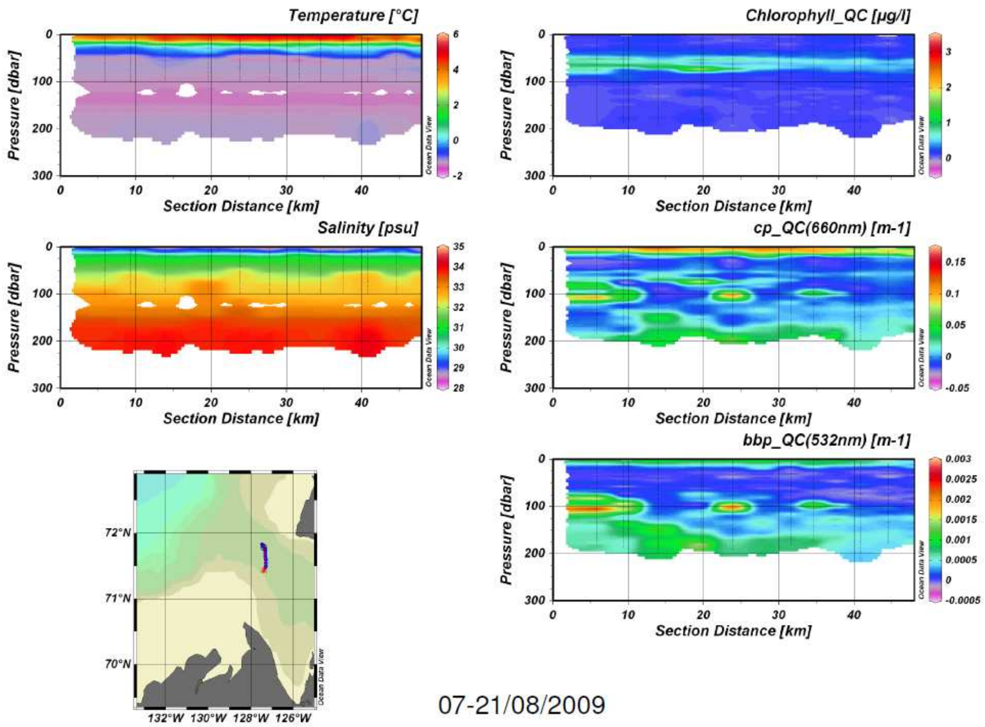

Figure 2: Temperature (℃), salinity (psu) and bio-optical profiles (chlorophyll-a in µg/l, beam attenuation coefficient at 660 nm (cp) in m^{-1}, particulate backscattering coefficient at 555 nm (bbp) in m^{-1}) recorded by the ProvBio float between surface water and 200 m depth in the Beaufort Sea. The measured bio-optical properties can be used as proxies for the concentrations of suspended particles and chlorophyll-a.

In July 2010, the signature of the Gironde plume was obvious within a 10 m thick surface layer in the adjacent coastal waters (Figure 4), resulting from a high river discharge in June. However, as the freshwater discharge significantly dropped in July, particles in suspension within the water column massively sank to form a thick and turbid bottom nepheloid layer extending up to 40 km offshore.

These first observations provided by the profiling floats clearly complement satellite observations limited t surface waters and highly affected by the cloud cover. ProvBio data first allow observing the deep chlorophyll maximum which can hardly be remote sensed in turbid coastal waters. Moreover, field measurements are the only way to observe the sinking of particles within the water column and track the transport of particles within the bottom nepheloid layer. While match-ups between satellite and ProvBio data are currently analyzed, these first deployments prove that the transport of suspended solids can be monitored in coastal waters directly influenced by river plumes by combining ocean color satellite data and field measurements recorded by autonomous profiling platforms.

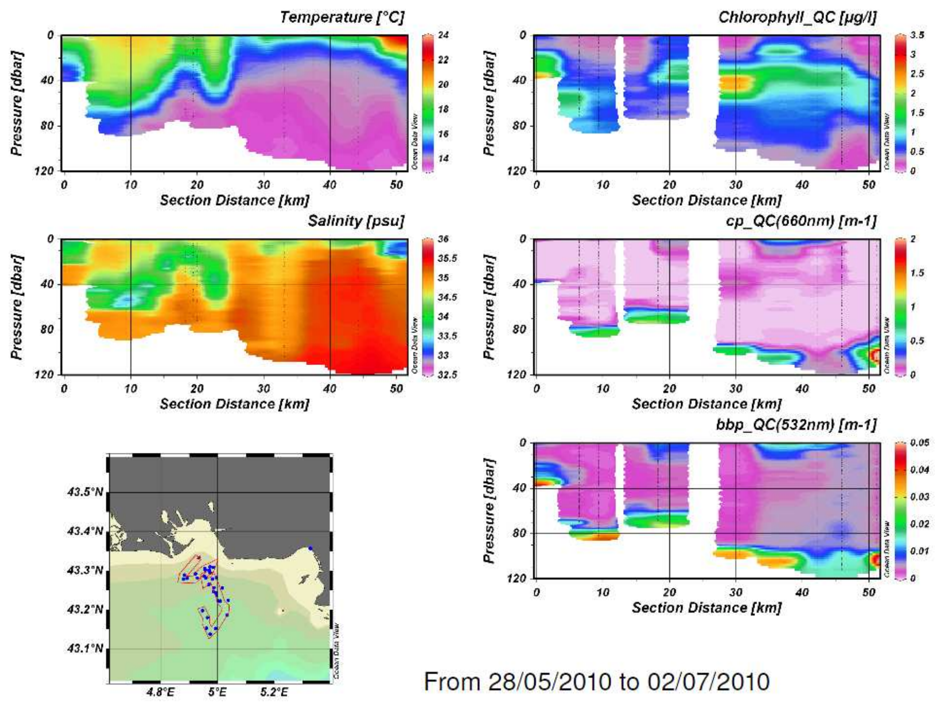

Figure 3: Typical Temperature (℃), salinity (psu) and bio-optical profiles (chlorophyll-a in µg/l, beam attenuation coefficient at 660 nm (cp) in m^{-1}, particulate backscattering coefficient at 555 nm (bbp) in m^{-1}) recorded by the ProvBio float between surface water and bottom in the Rhone River plume (second deployment). The measured bio-optical properties can be used as proxies for the concentrations of suspended particles and chlorophyll-a.

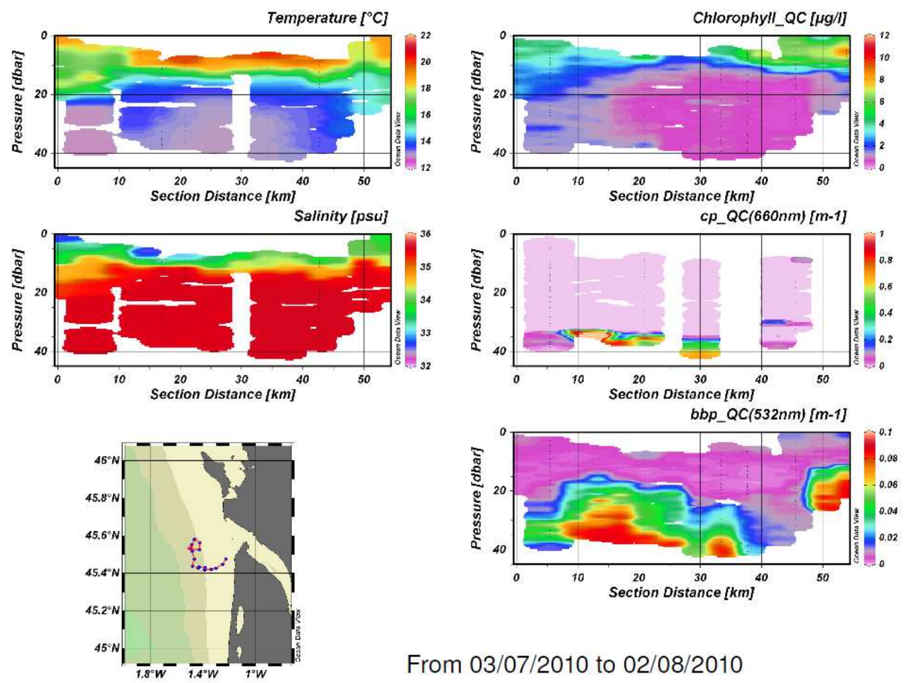

Figure 4: Typical Temperature (℃), salinity (psu) and bio-optical profiles (chlorophyll-a in µg/l, beam attenuation coefficient at 660 nm (cp) in m^{-1}, particulate backscattering coefficient at 555 nm (bbp) in m^{-1}) recorded by the ProvBio float between surface water and bottom in the Gironde River plume (second deployment). The measured bio-optical properties can be used as proxies for the concentrations of suspended particles and chlorophyll-a.

Conclusions

This study tried for the first time to prove the capability of autonomous bio-optical floats, namely the ProvBio originally designed for the open ocean, in coastal waters directly influenced by river inputs. Five deployments and recoveries have been successively achieved in the margins of Arctic and European rivers margins. Despite several technical problems (intense bio-fouling, rapid offshore drifting, regular ship assistance and interaction with fishery activities), physical and bio-optical data of quality were carried out using the ProvBio floats which proved to greatly complement satellite observations and field measurements carried out onboard oceanographic vessels. Future deployments planned in 2011 in the Rhone and Amazon River plumes are expected to confirm these first results in order to develop an operational monitoring system able to document the three-dimensional dynamics of suspended particles in coastal waters.

Acknowledgements

The authors want to thank the crew members of the Amundsen (CCGS) and Antédon II (CNRS-INSU) research vessels and G. Oggian (UMR 5805) for their help when deploying and recovering the ProvBio floats. This study was funded by the Groupe Mission Mercator Coriolis and the Centre National d’Etudes Spatiales.

References

Dagg, M., Benner, R., Lohrenz, S. and D. Lawrence, 2004. Transformation of dissolved and particulate materials on continental shelves influenced by large rivers: plume processes. Continental Shelf Research, 24, 833-858.

Doxaran, D., Froidefond, J.M., Lavender,S.J. and P. Castaing, P., 2002. Spectral signature of highly turbid waters. Application with SPOT data to quantify suspended particulate matter concentrations. Remote Sensing of Environment, 81, 149-161.

Doxaran D., J.M. Froidefond, P. Castaing and M. Babin, 2009. Dynamics of the turbidity maximum zone in a macrotidal estuary (the Gironde, France): Observations from field and MODIS satellite data. Estuarine, Coastal and Shelf Science, 81, 321–332.

Eisma, D., Bernard, P., Cadée, G.C. Ittekkot, V., Kalf, J., Laane, R., Martin, J.M., Mook, W.G., van Put, A. and A. Schuhmacher, 1991. Suspended-matter particle size in some West-European estuaries; part II: A review on floc formation and break-up. Netherlands Journal of Sea Research, 28, 215-220.

Geyer, W.R., Hill, P.S. and G. Kineke, 2004. The transport, transformation and dispersal of sediment by buoyant coastal flows. Continental Shelf Research, 24, 927-949.

Le Reste, S., André, X., Claustre, H., D'Ortenzio, F. and A. Poteau, 2009. First success of ProvBio floats. Coriolis NewsLetter, 5, 5-8.

Schlunz, B. and Schneider, R.R., 2000. Transport of terrestrial organic carbon to the oceans by rivers: re-estimating flux and burial rates. International Journal of earth Sciences, 88, 599-606.

Empirical correction of XBT fall rate

By Mathieu Hamon[1], Pierre-Yves Le Traon[1] and Gilles Reverdin[2]

[1] Laboratoire d'Océanographie Spatiale, IFREMER, Plouzané, France
[2] LOCEAN, Paris, France

Abstract

We used a collocation method between XBT and CTD/OSD (Ocean Station Data including bottle cast and low resolution CTD) from World Ocean Database 2005, hereafter WOD05 (Levitus et al. 2005) (1◦×2◦×15 days) to statistically correct the XBT fall rate. An analysis of the annual median bias on depth showed that it is necessary to apply a thermal correction linked to probe calibration error, a second order correction on the depth as well as a depth offset representing measurement errors during XBT deployment. We had to separate data in several categories: shallow and deep XBT and deployment sea temperatures (below or above 10◦ C).We also processed separately XBT measurements close to Japan between 1968 and 1985 due to large regional biases. Once the corrections have been applied, the analysis of heat content signal is derived from corrected XBT. From this analysis, we confirm that the maximum heat content in the top 700 meters found during the 70's in early papers (Wijffels et al. 2008; Levitus et al. 2009) can be explained by the XBT biases. In addition, a trend of 0.32 x 10^{22}J/year is observed between the period 1970 and 2008.

Introduction

Identifying and quantifying the effects of global warming is one of the most important research areas for the international oceanographic community. Due to its heat capacity, much larger than the other elements of the climate system, it is estimated that the oceans have absorbed more than 80% of the earth warming due to the anthropogenic increase of greenhouse gas concentration (Levitus et al. 2001 and 2005). In the last few years, many studies have tried to accurately determine the evolution of the global ocean heat content (e.g. Gouretski and Koltermann, 2007; Wijffels et al. 2008; Levitus et al. 2009). They observed biases between the different instruments used to collect ocean temperature profiles. Expendable BathyThermographs (XBT) have been mostly launched from underways ships since 1966 allowing the measurement of the upper ocean's temperature.

The XBT system does not directly measure depth. The accuracy of the depth associated with each temperature depends on an equation which converts the time elapsed since the probe entered the water to depth. Gouretski and Koltermann (2007) used an ocean climatology based on high quality data (Conductivity Temperature Depth (CTD) and Nansen casts) to identify biases in XBT observations. They found a positive bias by 0.2 − 0.4◦C on average with some variations from year to year. Based on this study and further comparisons between data types, Wijffels et al. (2008) (hereafter W08) proposed a yearly linear correction on the depth. More recently Levitus et al. (2009) used a simpler temperature correction, subtracting to all XBTs, the annual median temperature bias compared on a CTD climatology. Based on these previous studies, Gouretski and Reseghetti (2010) proposed a new correction using a depth correction added to a temperature offset. The W08 correction is a reference for the processing of XBT data but one can question whether this correction depends on the method of comparison between XBT and CTD profiles. A new more precise correction, correcting individually each type of XBT cannot be envisioned but, is it also possible to refine the W08 correction? The objective of this paper is to build a new correction based on the precise observation of the bias derived from collocated XBT and CTD/OSD (Ocean Station Data) data.

Data and collocation method

In the current study we used temperature profiles of the World Ocean Database 2005 (hereafter WOD05) (Levitus et al. 2005) where profiles have been interpolated to standard levels. The ocean was subdivided into 16 vertical levels from the surface to 700m depth. We used profiles that have been processed when identification was possible using the correction H95 (Hanawa et al. 1995). Instead of using two climatologies, one constructed with CTD and bottles profiles, and the other with XBT profiles, we used a collocation method to compare instruments. We selected all CTD and OSD geographically distant by less than 1◦ of latitude and 2◦ of longitude and temporarily distant from less than 15 days. For each individual XBT profile, we calculated a reference profile as the median of all CTD and OSD profiles selected in the region of collocation.

The bias profile was then calculated by subtracting this reference profile from the XBT profile. Following Levitus et al. (2009) median rather than arithmetic average was used, as it reduces the influence of outliers. Moreover, we removed XBT profiles shallower than 200m depth to exclude coastal regions. This method allows us to retain about 104 profiles a year between the year 1967 and 2007.

Test of the W08 correction

The W08 correction A is a linear correction computing the "true" estimated XBT depth Ztrue from the depth Z calculated with the original fall rate (equation 1).

$$\text{Ztrue} = Z(1-A) \qquad (1)$$

W08 separated on the one side the deep XBT profiles (hereafter called XBTD) measuring temperature below 500m (in standard levels) which are predominantly T7 or Deep Blue, and on the other side, shallow XBT profiles (hereafter called XBTS) which are predominantly T4 instruments. According to their study, W08 note a depth error near 400 m of 10 m for XBTS and half that for XBTD on average. We first applied the W08 correction to our collocated profiles.

Figure 1 shows the yearly raw and W08 corrected median bias on depth as a function of year. According to Gouretski and Koltermann (2007) and Wijffels et al. (2008) there is a positive bias between vertically averaged XBT temperature and high quality data like CTD and OSD. This median bias varies with the year of deployment of the XBT. It varies between 0.2◦ C and 0.1◦ C during the end of the 60's until the beginning of the 80's. Then the bias stabilizes around 0.05◦ C. Moreover this evolution agrees with the results of Levitus et al. (2009). The vertical median bias is not uniformly reduced while applying the W08 correction. Obviously the linear correction does not correct the surface bias (Figure 2). It can also be sometimes too large and induce a negative bias. Our comparison method thus suggests that a linear correction is not sufficient to properly reduce the observed biases.

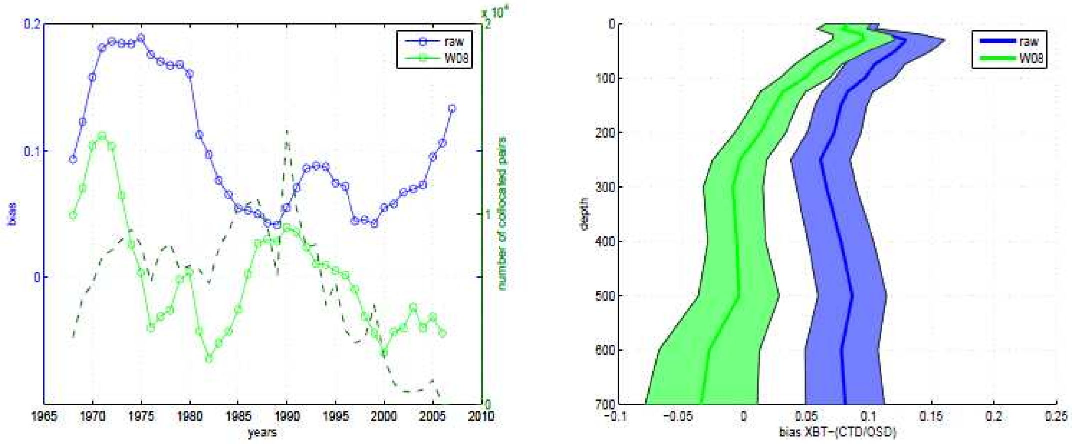

Figure 1: (Left panel) Evolution of XBT-CTD 0/700m median raw bias (blue) and corrected by W08 (green) integrated between 0 and 700m (°C). The number of yearly collocated pairs is indicated with the green dotted line. (Right panel) Median raw bias (blue) and corrected by W08 (green) as a function of depth averaged over the study period. The width represents the standard deviation of the annual median bias (°C).

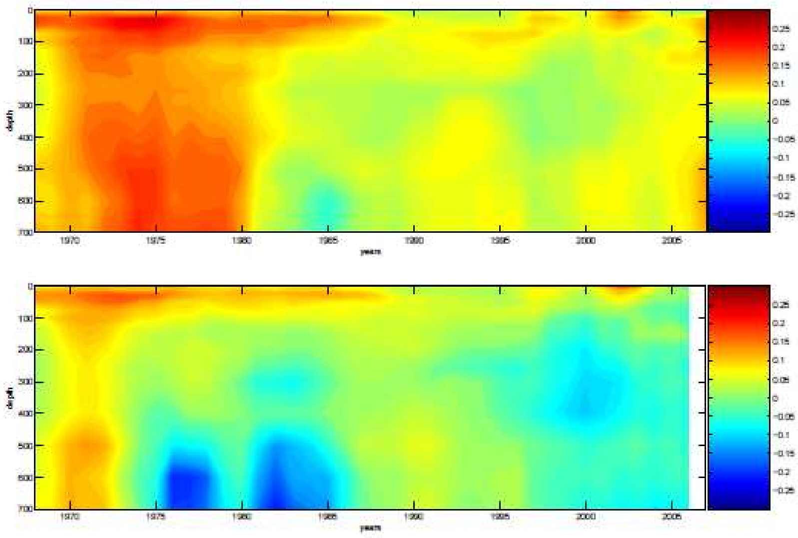

Figure 2: Evolution of XBT-CTD median raw bias (°C) (Top panel) and corrected by W08 (Bottom panel) as a function of depth (in meters) and time (years).

Analysis of the XBT bias

We will try to refine the model of bias correction by examining in more detail the vertical and spatial structure of the XBT/CTD biases. The W08 correction does not properly reduce the global median bias of our XBT and CTD/OSD collocation. We begin to compare very close pairs with weak temperature gradients and we identify a thermal bias. This observation agrees well with the recent work of Gouretski and Reseghetti (2010). We then computed the median annual bias as a function of depth to adjust at a given temperature the depth indicated by the original fall rate. We can linearly interpolate to retrieve the temperature at standard levels. We compute the depth bias at each standard level with the first order approximation (see equation 2).

$$dZ = (TCTD-TXBT)\ \delta Z/\delta TCTD \qquad (2)$$

Our calculations of depth bias from collocated profiles points to several observations. As in Wijffels et al. (2008), the behavior of XBTS and XBTD was different. Moreover, the collocated profiles do not seem to be corrected by a linear function, but rather by a parabolic function. This parabolic character is more or less pronounced according to year, geographical area and the type of XBT. We thus computed a second order correction with a least square fitting process for all years of deployment and all classes of XBT made in this study. The bias on depth also has a different behavior in the first meters of the probe fall. Between the surface and 30m, the error deviates from its parabolic behavior, possibly due to the high variability of surface temperature added to low gradient of the surface mixed layer producing high variability in the calculated dZ quantities. On the other hand, there seems to be a correlation between depth bias and the temperature of the sea water where the probe had been deployed (Thadathil et al. 2002).

Figure 3 shows the depth bias at 100m as a function of average temperature between 0 and 200m for XBTS (in red) and XBTD (in blue) averaged over the studied period. We notice an increase of the bias toward low temperatures, without finding a different behavior between the two classes of XBT. Although, Figure 3 still illustrates the need to process XBTs in categories of temperatures, nothing clearly distinguishes XBTS from XBTD at this depth. Comparing the bias at a given depth is not a sufficient indicator as it is the behavior of the depth error that is essential.

Figure 4 represents the linear part (Az) as a function of the parabolic part at 400m depth (Bz2) for a new correction for XBTS (circles) and XBTD (stars) at high temperature (left) and at low temperature (right). Each dial represents a different regime of the yearly median depth bias. Most profiles have to be corrected by a function having a negative parabolic part and a positive linear part. This indicates that the fall rate equation of most XBT probes badly estimates the actual speed of fall in the first meters and tends to approach it at greater depth. At lower temperatures, the behavior of XBTS and XBTD fall is totally different. Particularly in the end of the 70's and the 90's, we notice that the parabolic part of the XBTD becomes positive and several profiles have a negative linear part. Furthermore, we note that those probes need more different regimes of correction than the others.

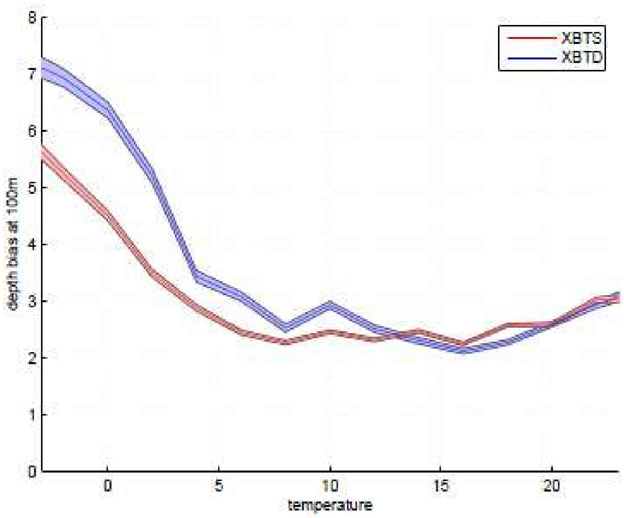

Figure 3: Median XBT-CTD depth bias at 100m (℃) de pth as a function of the integrated temperature between 0 and 200m depth for XBTS (red) and XBTD (blue). The standard deviation divided by the square root of the number of selected pairs in each class is represented with the colored area.

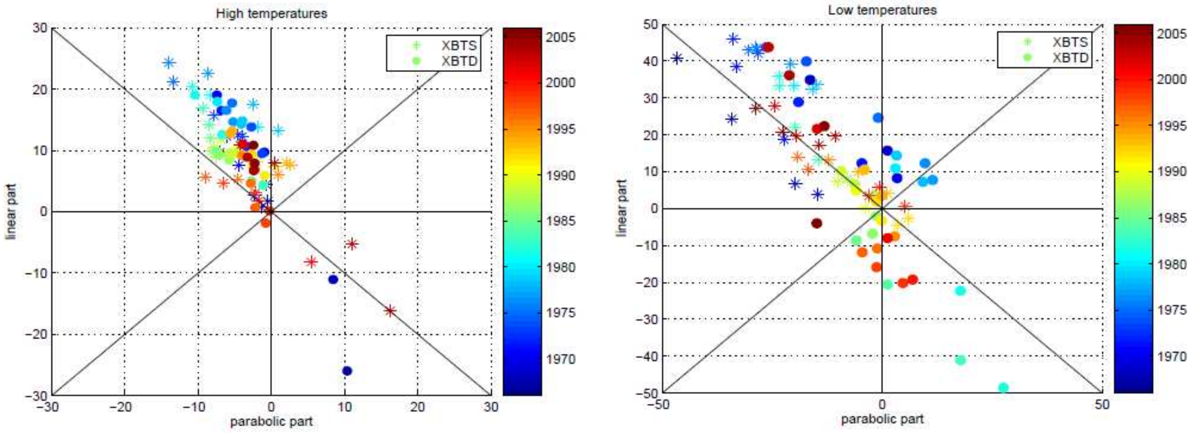

Figure 4: Linear part (coefficient B(t)) an a function of parabolic part (A(t)×400) at 400m depth for XBTS (large dots) and XBTD (stars). The left figure represents XBTs deployed at high temperatures. The right figure represents XBTs deployed at low temperatures. Years are indicated with the colorbar.

A new correction

Based on the previous analysis, we propose the following new correction for XBTs (equation 3 and 4):

1. Correction of thermal bias:

$$TXBT = TXBT - Toff \qquad (3)$$

2. Correction of the depth bias:

$$Ztrue = Zobs\,(1-A-BZobs) - Zoff \qquad (4)$$

Thermal correction

Errors on the calibration of the temperature probes can also be a source of bias. In addition, as the XBTs are passive sensors, the possibility of parasites resistances or other circuit dependent parameters can induce errors in the temperature data reported by the instrument. Comparing neighboring XBT and CTD/OSD profiles in the upper mixed layer, we observed a positive thermal bias between 10m and 30m. Following Gouretski and Reseghetti (2010), we selected close profiles with a weak temperature gradient in the upper layer (less than 0.0025◦C/m). This criterium guarantees that the observed bias is not related to the estimation of the depth of the XBT probe but to an error of calibration.

As we did not find significant differences between profiles measured in high or low water temperature, we decided to separate them only in two categories. We compute an offset Toff related to XBTS and another for XBTD (equation 5). The thermal offset associated with XBTS is largely positive between 1968 and 1980 (0.069◦C in average) and tends to zero afterward. The thermal bias of XBTD is more constant. A maximum is reached before 1980 (0.040◦C in average) which decreases during the 80's and becomes again maximum at the end of the 90's (0.047◦C in average between 1995 and 2005).

Second order correction

The parabolic character of the correction is certainly due to a too simple approximation of the XBT fall rate. Indeed, it is possible that the first XBT fall rates calculated by observation of the fall of a probe in a water tank were not adapted to forecast their behavior in ocean water associated to variations of temperature and salinity. Furthermore, characteristics of probes can vary in time. The weight and all hydrodynamic parameters are essential to estimate the velocity of probes. According to Seaver and Kuleshov (1982), a weight uncertainty of 2% could induce 8.8m of depth error at 750m. Gouretski and Reseghetti (2010) find significant weight variations for probes manufactured after 1992 and we can easily extrapolate those results to earlier probes.

All these error sources imply that the XBTs do not fall exactly as a second order equation of the time, and this equation might also change with time. Following a global approach, we chose to differentiate several profile categories, XBTS and XBTD deployed in high or low temperatures (above or under 10◦ C) to optimally correct the database. This distinction allows us to have a sufficient number of profiles in each category, guaranteeing certain robustness in our calculations (Figure 5). To avoid discontinuities between profiles deployed in water close to 10◦ C, we used an overlap. For the high temperatures class, we selected all XBTs deployed in water warmer than 8◦ C and for the low temperature class, we selected XBTs deployed in water colder than 12◦ C.

We applied the process of depth correction three times because of the difficulty to exactly calculate the median depth bias, particularly in the areas of weak thermal gradients.

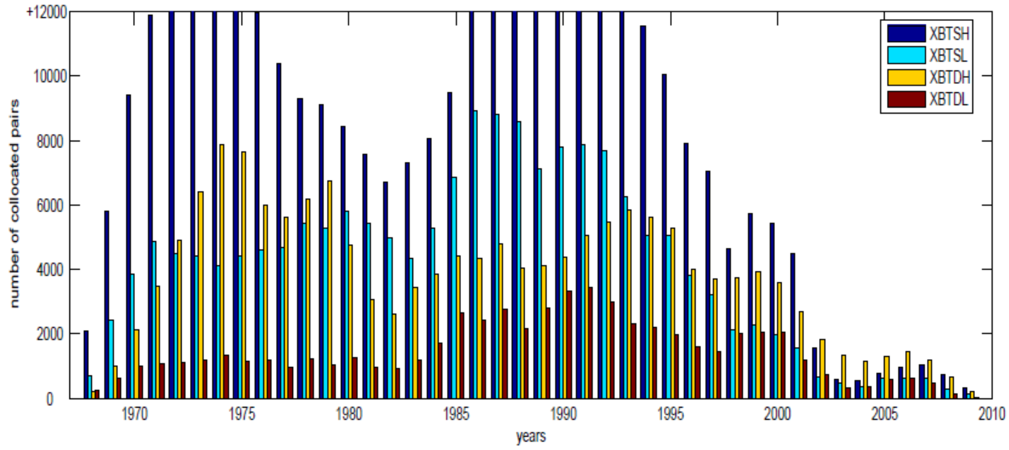

Figure 5: Number of colocated pairs for the four classes of XBT as a function of time. XBTS(D)H/XBTS(D)L correspond to shallow (deep) XBTs deployed in high and low temperatures.

Depth offset

In spite of a good correlation between the median bias and its yearly correction, the resulting temperature bias is not zero, particularly in the surface layer. This is due to a median offset not corrected by the second order correction because it is poorly observed by our depth bias calculation involving the local gradient of temperature. There is not a clear physical explanation for this offset, but it could result from human mishandling. Probes launched from surface ships do not touch vertically the water surface and take time to sink at the assumed fall speed. Their initial velocity may also be questioned. The calculation of the drop height in board is very rough because of movements on the ocean surface as the swell or waves. All these phenomena prevent us to accurately characterize a median offset.

To overcome this lack of information, we opt for an empirical fitting proportionally adjusting the offset with the pre-corrected bias by the parabolic function. We used more exactly the yearly median depth error between 30m and 100m to statically correct the depth offset error. We chose to compute the offset in this thin layer because it corresponds to a compromise between the choice of a surface layer, where the calculation of a depth bias is not influenced by the fall rate error and the layer of maximum gradient (equation 5).

$$Zoff = \langle dZ \rangle 30\text{-}100 \qquad (5)$$

We note that the depth offset can be negative for several years. This could occur when the entry of the probe in water is detected late or if the speed of the probe at the impact in water is too high. In those cases the reported depth can be really deeper than the observed depth.

Specific case

After the global bias analysis by collocation, it is possible that residual biases identified may result from high spatial variations, as it is for example the case in the Kuroshio or Gulf Stream region, due to sampling issues. Measurements close to Japan and in the western Pacific basin (the northwest Pacific region bounded by 180◦ E and north of 20◦ S) show a strong negative corrected bias that appears during the period 1968/1985 after the global correction. We note a predominantly negative bias at 300m depth (Figure 6), which implies that these XBTs are poorly corrected by our global parabolic term. In this case, it is possible that the problem originates partially from specific XBT probes, but as we have not been able to identify them, this requires a specific regional correction. This distinction is particularly necessary because retaining these XBTs in the global dataset would have an impact on the estimated correction.

Thus, we separated these regional profiles in another category, thus increasing the robustness of the global correction. The coefficients A and B calculated for these particular XBTS are quite similar to those calculated for XBTS deployed in high temperature, whereas the coefficients for the XBTD in this region are very different from the others. The coefficient A is largely positive in the first years and decreases until 1985 and B is strongly negative and increases with time. The depth offset is also strong. This behavior is specific to those regional XBTD. The other difference is referred to the temperature offset. During the first years, the regional temperature offset is positive but not as strong as for the other XBTs. From 1975 it becomes slightly negative.

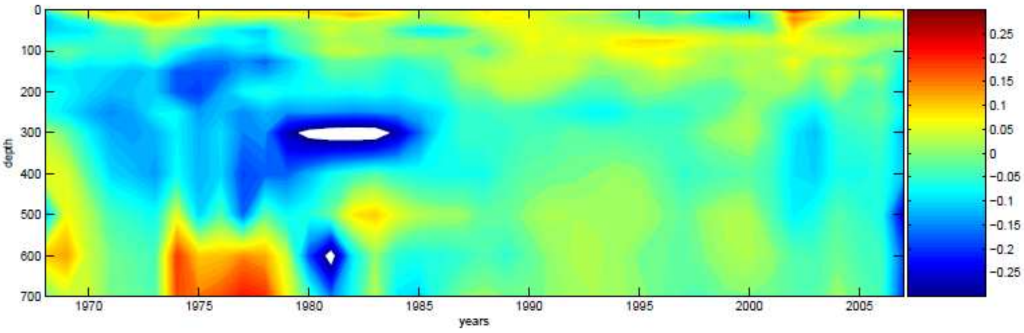

Figure 6: Evolution of XBT-CTD median bias (℃) deployed in the western Pacific basin (the region is bounded by 180◦ E and 20◦ S) between 1968 and 1985, corrected by a global parabolic correction, as a function of depth (in meters) and time (years).

Calculation of the corrected heat content

Following Wijffels et al. (2008) and Levitus et al. (2009), we also estimated a median depth bias on Mechanical BathyTermograph (MBT). The following figures result from the correction of both XBTs and MBTs. Using the same methodology we performed a second order correction added to an offset. We also separated MBT deployed at high and low temperatures. For those probes, the selected threshold was 12◦ C for the median temperatures calculated between the surface and 100m depth. With the globally corrected database, we can easily map the observations on a latitude and longitude grid (4◦×8◦). The annual mean anomalies of temperature are obtained by subtracting the WOA05 climatology (Levitus et al. 2005). We attributed to empty boxes the value of the annual mean anomaly of all full boxes.

Figure 7 shows the 0-700m integrated heat content calculated from the corrected XBT database (green), the raw XBT database (red), the entire WOD05 database (red) and the entire database where XBT and MBT have been corrected (blue). The calculation of the corrected heat content suggests that the local warming observed during the 70's was the result of the positive bias of XBT probes. On the other hand, we note that the global heat content calculated from corrected XBTs is very close to that calculated with the entire corrected database (such agreement is also found when considering specific layers like 0-400m or 400-700m) . This suggests that XBT data are now globally closer to CTD data. This new correction allows us to find a linear trend of global heat content of 0.32 x 10^{22}J/year between 1970 and 2008. Of course, this is strongly dependent on the assumption to fill missing boxes with the annual anomaly for that year, as much southern hemisphere boxes were not sampled in the early periods.

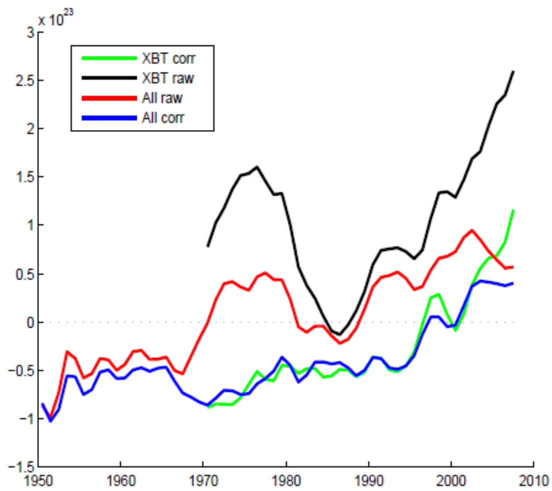

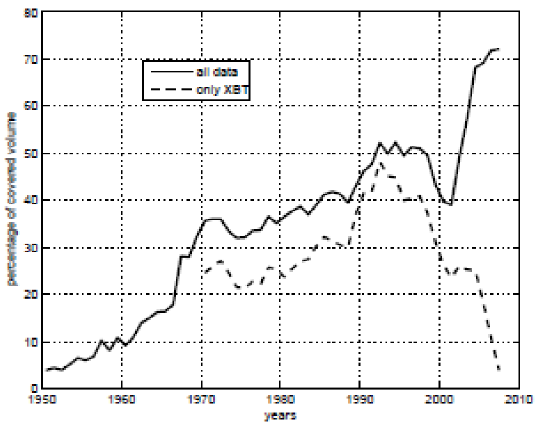

Figure 7: Integrated heat content (Joules) between the surface and 700m depth calculated using the entire raw dataset (red), the entire corrected dataset (blue), and only using raw XBTs (black) and corrected XBTs (green) function of years (Left panel). Percentage of the oceanic volume covered by 4◦×8◦ boxes including all data (full line) and only XBT data (dashed line)(Right panel).

Conclusions

We had to consider 6 different XBT classes to compute a globally second order correction on depth. We chose to separate XBTS and XBTD mostly related to T4 and T7 during the study period. We also separate XBTs deployed in cold or warm water (colder or warmer than 10◦C on average between the surface and 200m) due to the dependence of temperature on the behavior of the XBT probes. A parabolic correction was not sufficient, and it was necessary to apply offsets: One thermal offset only depending on the XBT type to apply to the temperature profiles and a second one, a depth offset.

Although we adopt a global perspective, we separated XBTs launched in the western Pacific basin between 1968 and 1985 because of their particular behavior. Our empirical approach does not attempt to found the reasons why those probes have a particular behavior but doing this exception allows to increase the robustness of our global correction. This specific case has also been discussed in W08. They found that the depth error at 400m was almost similar between the different basins except for the western Pacific region. As we also show here, they identify a regional negative error.

Furthermore, the thermal offset can be compared to the results obtained by Gouretski and Reseghetti (2010). Our analysis detects an offset almost two times smaller than theirs. This distinction is probably due to our selection criteria which is more stringent. We selected fewer profiles but only those with a thermal gradient lower than 0.0025◦C/m, whereas their upper limit is 0.005◦C/m. Despite the lower total number of profiles selected the calculation of the offset remains statistically accurate. We corrected the MBT database with the same methodology to obtain an entire corrected database. We were able to compute a revised 0-700m heat content and a corresponding estimate of a new linear trend. These calculations agree with other recent papers, thus supporting that the anomalous increase of heat content during the 70's originated from uncorrected XBT biases. It is now necessary to perform a more detailed analysis to highlight the potential gain of such a new correction on an entire database.

References

Gouretski V., K. Koltermann, 2007. How much is the ocean really warming? Geophysical Research Letters, Vol. 34, L01610. Doi: 10.1029/2006GL027834.

Gouretski V. and F. Reseghetti, 2010. On depth and temperature biases in bthythermograph data: Development of a new correction scheme based on analysis of a global ocean database. Deep-Sea Research I 57 (2010) 812-833.

Hanawa K., P Rual, R. Bailey. A Sy and M. Szabados, 1995. A new depth-time equation for Sippican or TSK T-7, T-6 and T-4 expendable bathythermographs (XBT). Deep Sea Research Part I: Oceanographic Research Papers, Vol 42, Issue 8, Pages 1423- 1451

Levitus S., J Antonov, and T. Boyer, 2005. Warming of the world ocean, 1955-2003. Geophysical Research Letters, Vol 32, L02604, doi: 10.1029/2004GL021592

Levitus S., J Antonov, T. Boyer, R.A. Locamini, H.E. Garcia and A.V. Mishonov, 2009. Global ocean heat content 1955-2008 in light of recently revealed instrumentation problems. Geophysical Research Letters, Vol 36, L07608, doi: 10.1029/2008GL037155.

Seaver G. A., S. Kuleshov, 1982. Experimental and Analytical Error of the Expendable Bathythermograph. Journal of Physical Oceanography, Vol. 12 592-600.

Thadathil P., A. K. Saran, V. V. Gopalakrishna, P. Vethamony, Nilesh Araligidad, Rick Bailey, 2002: XBT Fall Rate in Waters of Extreme Temperature: A Case Study in the Antarctic Ocean. J. Atmos. Oceanic Technol., 19, 391396.

Wijffels, Susan E., J. Willis, C. M. Domingues, P. Barker, N. J. White, A. Gronell, K. Ridgway, J. A. Church, 2008: Changing Expendable Bathythermograph Fall Rates and Their Impact on Estimates of Thermosteric Sea Level Rise. J. Climate, 21, 56575672. doi: 10.1175/2008JCLI2290.1

Geostrophic component of oceanic jets entering in the eastern Coral Sea observed with high-resolution XBT surveys (2008-2010)

By Christophe Maes[1], David Varillon[2], Alexandre Ganachaud[1], Florent Gasparin[1], Lionel Gourdeau[1], Fabien Durand[1]

[1] Laboratoire d'Etudes en Géophysique et Océanographie Spatiales (LEGOS) / Institut de Recherche pour le Développement (IRD), Centre IRD de Nouméa, BP A5, 98848 Nouméa cedex, Nouvelle Calédonie
[2] Unité de Service IMAGO / IRD, Centre IRD de Nouméa, BP A5, 98848 Nouméa cedex, Nouvelle Calédonie

Introduction

Before the development of ARGO program, subsurface temperature measurements have been mostly collected from eXpendable BathyThermograph (XBT) casts operated onboard commercial vessels as part of the Ship Of Opportunity Program (SOOP). The World Meteorological Organization and the UNESCO Intergovernmental Oceanographic Commission jointly support this program. SOOP addresses both operational and scientific goals to build a sustained ocean observing system and the first recommendation set recently by Goni et al. (2010) is to fully implement and sustain the XBT network. Undoubtedly linked to the maritime routes of the shipping industry that experienced large changes in the last decade, the XBT network still offers the potential of sampling regions that suffer from a deficit of in situ observations or, that require high-resolution data to complement the broad global scale ocean network.

This is typically the case for the Coral Sea and Solomon Sea that are at the heart of the Southwest Pacific Ocean circulation and Climate Experiment (SPICE) project. Ganachaud et al. (2007) set emphasis upon the transit of the south Pacific thermocline waters in the Coral and Solomon Seas that is potentially of great relevance for understanding the tropical climate variability and, for our ability to predict it. The geography of the southwest Pacific region is particularly complex (Figure 1) and large uncertainty on processes as well as on pathways of the water mass remains. As stated in the SPICE plan (Ganachaud et al., 2008a), the strategy to measure the South Equatorial Current (SEC) inflow in the Coral Sea is based on regularly repeated surveys between the northern tip of New Caledonia and the southern tip of Solomon Islands. The XBT data set collected by the SECARGO project since 2008 form the core of this effort for observing the characteristics of the SEC at the Coral Sea entrance.

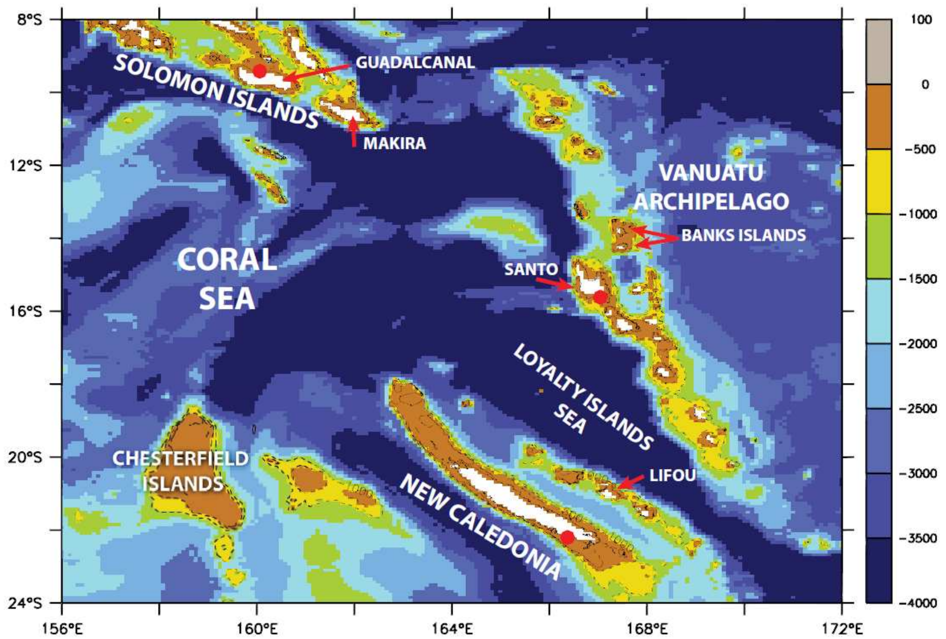

Figure 1: Geography and bathymetry of the eastern Coral Sea (dashed lines are the 500 and 1000 m isobaths). The red dots indicate the harbors (Nouméa, Luganville and Honiara) served by the commercial vessels.

Since the seminal modeling study of Webb (2000), our vision of the arrival of the SEC into the southwest Pacific Ocean profoundly changed from a picture of a broad and relatively weak westward current, as a part of the South Pacific subtropical gyre, to the description of narrow and intense jets strongly controlled by the topography of the region. In 2005, direct in situ observations based on a glider and a traditional oceanographic survey reveal the fine spatial characteristics of these jets (Gourdeau et al., 2008). At the entrance of the eastern Coral Sea, these observations also confirm the splitting of the SEC into a North Vanuatu Jet

(NVJ) and North Caledonian Jet (NCJ). A salient feature of the NCJ is its very narrow structure (typically 100 km wide) flowing westward off the northern edge of the New Caledonian reef (near 18°S). This result suggests that high- resolution observations are required to gain further understanding of the nature and variability of such jets. The relative geostrophic flow of the various jets entering the Coral Sea has been monitored by XBT observations thanks to the commercial line between New Caledonia and Solomon Islands via the Vanuatu archipelago (Figure 1).

Data and Quality control

As part of the SECARGO project, six surveys were operated between 2008 and 2010 (Figure 2). With the exception of one survey, the shipping route goes from New Caledonia to the harbor of Luganville in Santo Island (Vanuatu) via a passage south of Lifou (Loyalty islands). Then, the vessel joined the harbor of Honiara on Guadalcanal island (Solomon Islands) via the northeastern coast of Makira Island (Figures 1 and 2). The port calls in Vanuatu do not last more than two days, and the total sailing time of each survey does not exceed 5 days. The average speed of commercial ships is larger than 15 knots in open waters. In order to get a horizontal resolution of 1/3°, the observer embarked from Nouméa to Honiara operated a drop every 1.5 hour with a special attention paid to each beginning and ending parts of the survey.

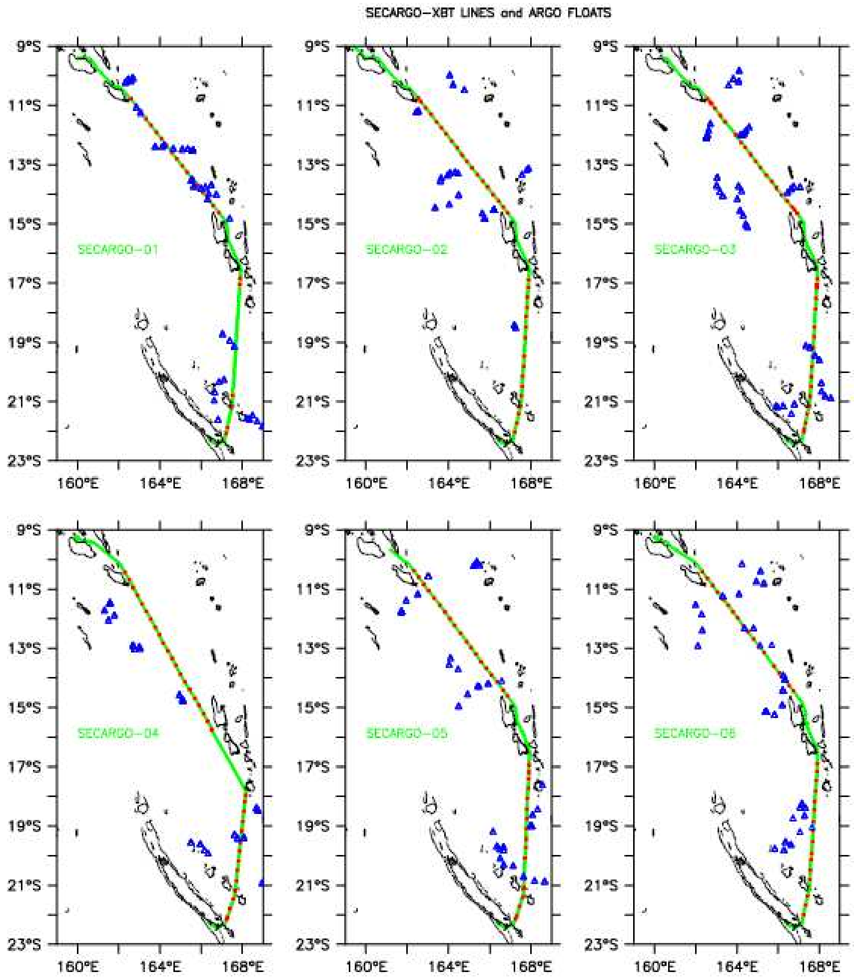

Figure 2: Ship tracks (green lines) and XBT cast locations (red squares) during the six surveys of the SECARGO project. The blue triangles indicate ARGO profiles collected within +/- 20-day of each survey.

The XBT probes used in the SECARGO project sample nominally down to 800 m for most of the types, reaching 2000 m for the specific T5-type (details are listed in the Table 1). However, the T5 probes require the vessel to slow down, a situation that could only be done occasionally. In the following, focus is set on the upper ocean variability down to 800-m depth. Hereafter, we analyze the various XBT drops section by section. No specific correction of possible thermal bias or fall rate equation is applied in this preliminary study. The quality control procedure consists in considering each temperature profile individually and visually comparing it with the closest nearby profiles. Profiles of dubious quality are rejected as well as profiles shallower than 400 m (i.e., the depth of the main thermocline). Some noisy structures were filtered out on a few profiles with a median filter on the vertical (at 15 or 25 m cutoff length). Isolated spikes (with depth interval less than 5 m) were removed manually and, finally, the surface values were replaced by the 10-m depth values. Finally, we compared all vertical temperature profiles with concomitant ARGO profiles (falling within a time interval of +/- 20 days for each specific survey – blue triangles on Figure 2). We discarded only a very small number of XBT casts which temperature values around 800 m were outside of the ARGO observed range. Finally, in the present study, we do intend to apply empirical corrections of XBT fall rate because the profiles have been collected over a short period of time, but this point will be considered in further studies to put into perspective the present data, especially, on long-term trends (Hamon et al., 2011, this issue).

SECARGO survey	Dates	Type of probes (nominal depth, in m)	Nb of profile (nb of used probes)
01	27 June – 01 July 2008	DeepBlue (760)	25 (26)
02	31 Oct. – 03 Nov. 2008	DeepBlue	35 (41)
03	27 Feb. – 03 March 2009	T5 (1830) and T7 (760)	40 (57)
04	18 Aug. – 20 Aug. 2009	T5, T7 and FastDeep (1000)	36 (43)
05	17 Feb. – 20 Feb. 2010	T5, T7 and FastDeep	39 (46)
06	22 Nov. – 25 Nov. 2010	T7	34 (44)

Table 1: Characteristics of the SECARGO surveys.

After the quality control procedures described above, the irregularly spaced casts were gridded in latitude (1/6°) and depth in order to obtain a uniform field of dynamic height anomalies. The profiles are interpolated first on the vertical grid of the CARS climatology (Ridgway and Dunn, 2003). We then used a seasonal T-S relation derived from the closest point found in CARS to estimate the salinity field associated with each temperature value before computing the dynamic height. Finally, the cross-track geostrophic currents and transports were calculated from the resulting along-track gradient of dynamic height.

In addition to XBTs, ARGO floats were released in 2008 (5) and in 2010 (5) in collaboration with the team of Pr. Steve Riser from the University of Washington. Based on the hypothesis that these floats would drift into the Coral Sea, which turned out to be valid at least in 2008, these floats provided unprecedented in situ observation in the region. All the commercial vessels have also collected of sea surface salinity observations from onboard thermosalinographs. In 2010, we also deployed surface drifters from the "Surface Velocity Program" equipped with salinity sensors within the context of the calibration/validation of the European SMOS mission (Boutin et al., 2010).

Main Results

For the purposes of this study, the casts are considered as two quasi-meridional sections between 22°S and 17°S, and between 15°S and 11°S (Figure 2). In their northernmost part, the temperature sections clearly exhibit the signature of the equatorial warm pool, with temperatures higher than 28°C in the upper 100 m (Figure 3). At the surface, seasonal variations range from 3 to 5°C and the waters always remain warmer than 25°C throughout the northern leg, in agreement with in situ coastal observations off Santo (Maes and Varillon, 2011). In the southern leg, temperature changes are much stronger and surface minimum near 20°C has been observed close to the coast of New Caledonia, in agreement with the CARS climatology. At depth, a strong vertical stratification associated with the main thermocline is seen between 100 m and 400 m depth. Below this latter depth, temperature falls down to 10°C in general. The position of the main thermocline (as delineated by the depth of the 16°C isotherm) exhibits a North-South tilt that is especially marked in the northern part of the section, i.e., between Vanuatu and Solomon Islands. In the southern part, the thermocline is deeper and less pronounced as expected for the South Pacific Ocean (Huang and Qiu, 1998). The SECARGO-02 and SECARGO-03 surveys show however an upward doming of the thermocline near 21°S, suggesting the presence of ocean eddies. Analysis of altimetric sea level anomalies confirms the presence of a cyclonic eddy between Lifou and Vanuatu at the time of the SECARGO-02 survey. This eddy has a strong signature in the relative geostrophic currents as shown below. Superimposed on these large-scale features, small-scale structures due to the presence of high frequency features remain. Nevertheless, detection of recurrent features suggested the presence of oceanic jets.

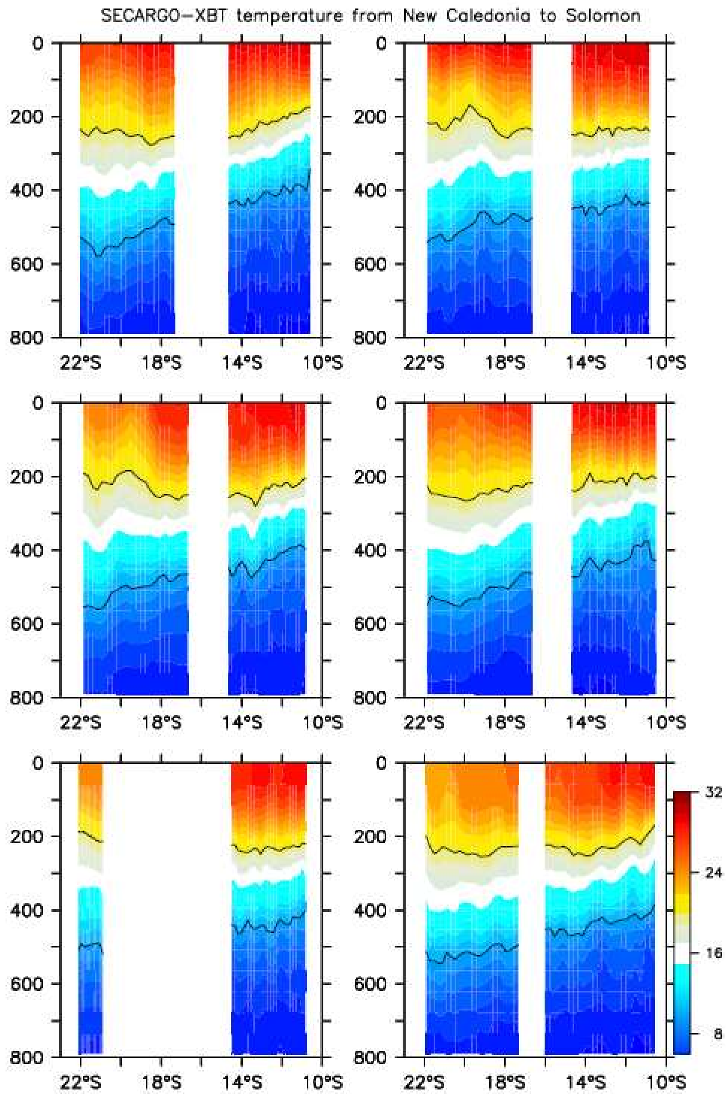

Figure 3: Vertical sections of temperature (in °C) as a function of latitude and depth (m) observed for each SECARGO survey (the black lines show the position of the 20°C and 10°C isotherms). The SECARGO-05 (left) and S ECARGO-03 (right) are shown in the top, the SECARGO-02 (left) and SECARGO-06 (right) in the middle and SECARGO-01 (left) and SECARGO-04 (right) in the bottom of the panel.

The cross-track relative geostrophic currents (referenced at 800 m) for each survey are displayed in Figure 4. The convention is to use warm color for eastward and cold color for westward flows. As expected, the general patterns are dominated by westward flows representing the arrival of the SEC into the Coral Sea and the resulting total integrated mass transport is found westward for each survey (Figure 5). An obvious feature of the sections is to exhibit a striation in current with typical horizontal length scale of 100 km order or less. Not surprisingly for rotating stratified fluids where jets are expected to occur spontaneously, direct observations of alternating zonal jets in the world ocean have been recently reported by Maximenko et al. (2005). In the case of the southwest Pacific Ocean, the occurrence of the jets is expected due to the blocking effect of the islands, even if some jets could be formed independently of the ocean topography (Kessler and Gourdeau, 2006). With the encounter of the Vanuatu archipelago, the SEC flow is deflected northward upon entering the Coral Sea, thereby forming the NVJ. This picture is nevertheless more complicated as shown by the presence of several jets in the 12°-14°S band (Figure 4) . Within less than 0.5° in latitude range, a westward flow is found at the northern the tip of Santo (near 14.5°S), and a second jet, which position is more variable in latitude, is mostly found around 12°S. This second jet corresponds to the flow deflected by the Banks Islands, located to the North-East of Santo (Figure 1). Northward of these jets, in the region between 12°S and the sou thern tip of Solomon archipelago (Makira island), alternating jets are found that correspond to the strong seasonal variability associated with the South

Equatorial Countercurrent (SECC) which has its center of action located near 9°S (Qiu and Chen, 2004). A strong eastward flow, southward of Santo, was also observed during the SECARGO-04 survey. This flow could be part of the Coral Sea Countercurrent (Qiu et al., 2009). It is probably associated with the complex re-circulation pathways of the NVJ in the region located between Santo and the northern reef of New Caledonia (Maes et al., 2007 ; Ganachaud et al., 2008b). In the southern leg, the intensity of the flows show comparable amplitude for all surveys, but with less well organized patterns. Moreover, the signature of cyclonic eddies in the second and third survey blurs the detection of other structures. Considering the recent work of Gasparin et al. (2011, submitted), we expected to find stronger evidence of the presence of the East Caledonian Current (ECC), a narrow and deep northwestward flow with a core extending down to at least 1000 m depth. Even if a prominently westward flow is found between 21°S and 19°S, it remains difficult to identify such a flow with the ECC in the absence of additional observations. It is also possible that the upper geostrophic shear of this jet is weaker, as compared to the NVJ, or that the present horizontal resolution, despite our efforts, is not sufficient. Other means needs probably to be used to overcome these difficulties and will be discussed later.

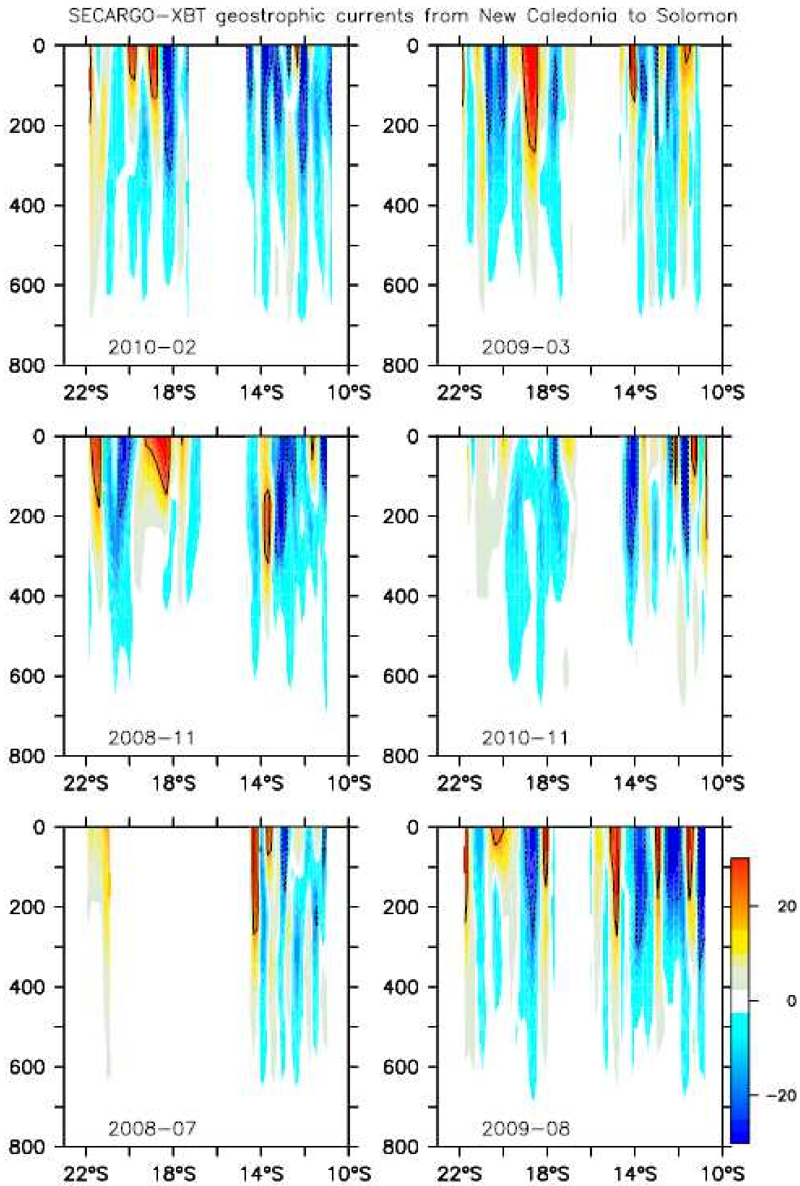

Figure 4: Vertical sections of cross-track relative geostrophic currents (in cm/s) as a function of latitude and depth (m) with the reference level set to 800 m depth. The full black line indicates the +20 cm/s isotach (eastward) and the dashed black line indicates the -20 cm/s isotach (westward). The order of the various surveys is similar to figure 3.

The integral of geostrophic cross-track velocity over 0-800 m from Makira to New Caledonia gives a cumulative transport ranging between -7 and -22 Sv (thus, entering the Coral Sea). These numbers should be compared to the estimate of -12 Sv for the 0-600 m geostrophic transport observed during a glider survey (Gourdeau et al., 2008), roughly along 162°E between Guadalcanal and the northern reef of New Caledonia (18°S). The nature of the sampling is very different between the glider survey that occurred over several months, and the XBTs that occurred in less than 5 days. Among the six SECARGO surveys, the variability is also quite different between the two legs. In the region between Solomon Islands and Santo, the total transport varied by a factor of 3, with two groups: -5 to -7 Sv for SECARGO 01-03-06 and -13 to -16 Sv for SECARGO 02-04-05. North of 12°S, three cases exhibit a weak eastward transport that could be probably associated with the SECC variability. South of 12°S, a consistent westward transport dominates and is slightly modulated by the presence of re-circulations flowing against the SEC. In the region between the Vanuatu and New Caledonia the situation is more complex with a stronger disparity (Figure 5). In one case (SECARGO-02), the transport is even found to be eastward for this particular leg, mainly due to the presence of one eddy in the region. In general, the contribution of the southern leg to the total transport is smaller than the one from the northern leg; in one case only (SECARGO-06), similar amplitude is found for the northern and southern component. Sensitivity tests done by Gourdeau et al. (2008) show that the transport of the NCJ could be divided by a factor of two depending of the choice of the level of no motion. The absence of a clear signature of the ECC in the second leg also suggests the possibility of an important geostrophic shear below 800 m depth.

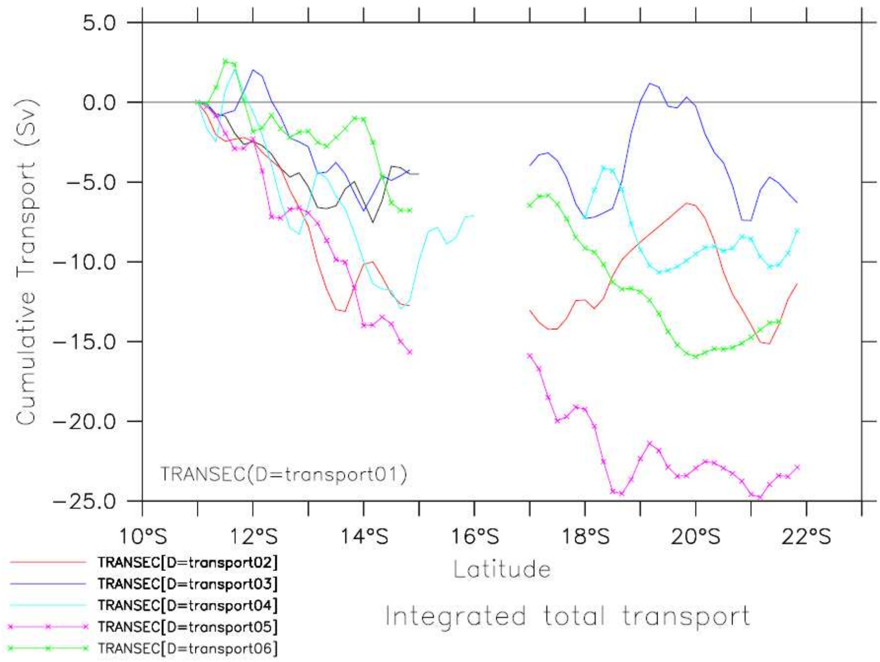

Figure 5: Cumulative cross-track geostrophic transport (in Sv) integrated southward along each survey of the SECARGO project (the blank zone in the middle corresponds to the Vanuatu archipelago where a null transport is assumed by the present study; note that no XBT casts were collected in the southern section during the first survey).

Discussion and perspectives

Within the SPICE context, an XBT line between Nouméa (New Caledonia) and Honiara (Solomon Islands) via the Vanuatu archipelago has been implemented since 2008, with a sampling twice a year. Based on the idea of closing the mass and heat budgets of the region (similar to the “Tasman box” of Roemmich et al., 2005), high-resolution XBT casts have been providing repeated measurements of the upper 800 m water column temperature. The above results provide the first opportunity to describe the fine spatial structures of the entire flow entering the Coral Sea, from the North (NVJ) to the South (encompassing the ECC which fate the NCJ near 18°S-163°E).

The features revealed by the present dataset raise the issue of the necessary referencing of geostrophic currents at a level deeper than the one reached by present XBT drops. It is likely that part of the geostrophic shear of the flow entering the Coral Sea occurs at depths greater than 800 m, particularly along the southern half of the section sampled here. Repeated glider surveys between Loyalty Islands and Vanuatu are currently being conducted to address this issue, and these results will be reported further.

Monitoring the upper density field and resulting geostrophic current flowing into the Coral Sea provides important information about the Coral Sea/Solomon Sea circulation system, particularly on the nature of the flow that subsequently crosses the Solomon Sea and eventually feeds the Equatorial Pacific Ocean. As a follow-up of earlier exploratory hydrographic surveys, the SECARGO XBT/Argo repeated surveys provide a new, important element of the Coral Sea monitoring system as planned by the CLIVAR/SPICE implementation plan (Ganachaud et al., 2008a).

Acknowledgments

This work benefits from the support of the GMMC and SHOM (thanks to Loïc Gourmelen and Nathanaële Lebreton). A special thank to Mr Adachi and its collaborators, and to the NYK-Hinode Company for their agreement of boarding the commercial vessels where we always find a very helpful welcome from the masters and their crew. We also address our gratitude to the agents of A.M.R.P.P (Agenge Maritime du Rond Point du Pacifique) at Nouméa. This work is co-funded by the INSU/LEFE IDAO “Solwara” project and ANR-09-BLAN-0233-01; it is a contribution to the CLIVAR/SPICE International programme.

References

Boutin, J., G. Reverdin, N. Martin, A. Lourenco, S. Morrisset F. Gaillard, J. Rolland, C. Maes, T. Delcroix, P. Blouch, 2010, Measurements of near-sea surface salinity (0-50 cm) using autonomous drifters, Proc. « ESA Living Planet Symposium », ESA SP-686.

Ganachaud, A., W. Kessler, S. Wijffels, K. Ridgway, W. Cai, N. Holbrook, M. Bowen, P. Sutton, B. Qiu, A. Timmermann, D. Roemmich, J. Sprintall, S. Cravatte, L. Gourdeau, T. Aung, 2007, Southwest Pacific Ocean Circulation and Climate Experiment (SPICE) - Part I. Scientific Background. NOAA OAR Special Report / International CLIVAR Project Office, CLIVAR Publication Series No. 111.

Ganachaud A., G. Brassington, W. Kessler, C.R. Mechoso, S. Wijffels, K. Ridgway, W. Cai, N. Holbrook, M. Bowen, P. Sutton, B. Qiu, A. Timmermann, D. Roemmich, J. Sprintall, S. Cravatte, L. Gourdeau, P. Eastwood, T. Aung, 2008a, Southwest Pacific Ocean Circulation and Climate Experiment. Part II. Implementation Plan. NOAA OAR Special Report / International CLIVAR Project Office, CLIVAR Publication Series No. 133.

Ganachaud, A., L. Gourdeau, and W. Kessler, 2008b, Bifurcation of the subtropical south equatorial current against New Caledonia in December 2004 from an hydrographic inverse box model, J. Phys. Oceanogr., 38, 2072-2084.

Gasparin, F., A. Ganachaud, and C. Maes, 2011, A western boundary current east of New Caledonia: observed characteristics, submitted to Deep Sea Research.

Goni, G., D. Roemmich, R. Molinari, G. Meyers, C. Sun, T. Boyer, M. Baringer, V. Gouretski, P. Di Nezio, F. Reseghetti, G. Vissa, S. Swart, R. Keeley, S. Garzoli, T. Rossby, C. Maes, and G. Reverdin, 2010, The Ship Of Opportunity Program, in Proceedings of OceanObs’09: Sustained Ocean Observations and Information for Society (Vol. 2), Venice, Italy, 21-25 September 2009, Hall, J., Harrison, D.E. & Stammer, D., Eds., ESA Publication WPP-306, doi:10.5270/OceanObs09.cwp.35

Gourdeau, L., W. S. Kessler, R. E. Davis, J. Sherman, C. Maes, E. Kestenare, 2008, Zonal jets entering the Coral Sea, J. Phys. Oceanogr., 38, 715-725.

Hamon, M., P.-Y. Le Traon, and G. Reverdin, 2011, Empirical correction of XBT fall rate, MERCATOR-CORIOLIS-Newsletter #41 (this issue).

Huang, R. X., and B. Qiu, 1998, The structure of the wind-driven circulation in the subtropical South Pacific Ocean, J. Phys. Oceanogr., 28, 1173–1186.

Kessler, W. S., and L. Gourdeau, 2006, Wind driven zonal jets in the South Pacific Ocean, Geophys. Res. Lett., 33, L03608, doi:10.1029/2005GL025084.

Maes, C., L. Gourdeau, X. Couvelard, and A. Ganachaud, 2007, What are the origins of the Antarctic Intermediate Waters transported by the North Caledonian Jet?, Geophys. Res. Lett., 34, L21608, doi:10.1029/2007GL031546.

Maes, C., and D. Varillon, 2011, Large-scale climatic and oceanic conditions around Espiritu Santo, in Natural History of Santo, P. Bouchet, Hervé Le Guyader and Olivier Pascal Eds, Éditions MNHN, Collection Patrimoines naturels, 49-53.

Maximenko, N. A., B. Bang, and H. Sasaki, 2005, Observational evidence of alternating zonal jets in the world ocean, Geophys. Res. Lett., 32, L12607, doi:10.1029/2005GL022728.

Ridgway, K. R., and J. R. Dunn, 2003, Mesoscale structure of the mean East Australian Current system and its relationship with topography. Prog. Oceanogr., 56, 189–222.

Roemmich, D., J. Gilson, J. Willis, P. Sutton, and K. Ridgway, 2005, Closing the time-varying mass and heat budgets for large ocean areas: The Tasman Box, J. Clim., 18, 2330–2343, doi:10.1175/JCLI3409.1.

Qiu, B., and S. Chen, 2004, Seasonal modulations in the eddy field of the South Pacific Ocean. J. Phys. Oceanogr., 34, 1515–1527.

Qiu, B., S. Chen, and W. S. Kessler, 2009, Source of the 70-day mesoscale eddy variability in the Coral Sea and the North Fiji Basin. J. Phys. Oceanogr., 39, 404-420.

Webb, D. J., 2000, Evidence for shallow zonal jets in the South Equatorial Current region of the southwest Pacific. J. Phys. Oceanogr., 30, 706–720.

Collecting and gridding complementary in-situ SST/SSS data for the calibration and validation of SMOS

By Emilie Brion[1], Fabienne Gaillard[1], Loïc Petit de la Villéon[2], Thierry Delcroix[3], Gaël Alory[3], Gilles Reverdin[4]

[1]LPO/IFREMER-CNRS-UBO-IRD, Plouzané, FRANCE
[2]SISMER/IFREMER, Plouzané, France
[3]LEGOS, Toulouse, France
[4]LOCEAN, UMR 7159 CNRS / IRD / Université Pierre et Marie Curie/MNHN / Institut Pierre Simon Laplace, PARIS, France

Introduction

Providing reliable in-situ surface temperature and salinity data over the global ocean within short delay is critical for the calibration and validation of the recently launched Soil Moisture and Ocean Salinity Satellite (SMOS). The work presented here has been undertaken as a contribution to GLOSCAL (Global Ocean Surface Salinity Calibration and Validation), retained as one of the ESA CalVal Projects. Based on the Coriolis datasets and using In Situ Analysis System (ISAS) tool, a near real time analysis system has been developed. It provides gridded fields of sea surface salinity and temperature and the corresponding in-situ dataset. In addition to research activities, these products would be used to help the quality control of SMOS satellite data, and to improve the algorithms and monitor sensor drifts and biases.

Dataset: Temperature and Salinity

The in-situ observations used to build our dataset are collected and processed by the Coriolis data centre. The main data provider is the Argo international array of profiling floats that reached its nominal coverage of the global ocean at 3°resolution at the end of 2007. Argo profilers report Temperature and Salinity when ascending from their deepest diving level (nominally 2000m) to a near surface level. To preserve the conductivity cell, the near surface measurement is performed at 4 or 5m (sometimes 10m) below surface, and this measurement can be a local sampling or a layer average. More isolated measurements from CTDs, sensor equipped marine mammals and moorings (such as TAO/PIRATA in the tropics) complement the dataset but provide little information on the surface levels. Within the context of GLOSCAL, we intent to incorporate data from surface dedicated instruments that are not yet in the Coriolis standard data flow. At present time, the only surface dataset providing global coverage for salinity is the network of Thermosalinographs (TSG) coordinated within the Global Ocean Surface Underway Data international program (GOSUD, http://www.coriolis.eu.org/Observing-the-ocean/Observing-system-networks/GOSUD). Newly developed drifting buoys equipped with conductivity sensors appear as a promising complementary system, but they remain at the moment limited to a few areas. We have thus focused on the French contribution to the TSG dataset. The method developed here will be extended later to TSG datasets from other contributors and to the drifting buoys data.

The Coriolis Near-real time dataset

The Coriolis Data Centre performs real time quality controls in two steps. First, a set of automatic tests (location and date, spikes...) is applied to the database, followed by a visual checking. The result is that quality flags ranging from 0 (no control) to 9 (missing value) (see Table 1) are assigned to each individual measurement. Then, after running daily objective analysis, a diagnostic test detects outliers by screening the analysis residuals. Anomalous profiles are visually checked by an operator. The Coriolis Processing is described in Coriolis report-04-047 (Coatanoan and Petit De La Villeon, 2005). For the needs of GLOSCAL, Coriolis data centre has implemented a near-real time data flow. At the beginning of each month, a new analysis is performed with the data of the pevious month. It should be noted that for this purpose, Coriolis uses ISAS version 5.2 for objective analysis (Gaillard, et al. 2009a). For the work presented here, we have developed a new version (V6.beta) that takes into account TSG data and includes some minor corrections.

Code	Meaning
0	No QC was performed
1	Good data
2	Probably good data
3	Bad data that are potentially correctable
4	Bad data
5	Value changed
6	Not used
7	Not used
8	Interpolated value
9	Missing value

Table 1: Quality flags used at Coriolis Data Centre

The thermosalinograph datasets

Sources of data

The TSG data are collected within the context of GOSUD international project. The GOSUD dataset is hosted by Coriolis that performs the project agreed real time quality controls on this dataset. For our analysis, only data that have passed delayed mode processing are used. For that reason we limit our selection to the fleet of commercial ships (managed by the ORE-SSS (Sea Surface Salinity Observation Service, http://www.legos.obs-mip.fr/observations/sss/)) and the French research vessels, all transmitting their data in real time. The instruments are rigorously calibrated by the sensor manufacturers or by the SHOM (Service Hydrographique et Océanographique de la Marine) following the Coriolis recommendations (Reverdin et al. 2006). Water samples collected aboard at regular intervals are analyzed in order to infer and correct the salinity drift due to the fouling and/or scouring that may occur. In addition to the water sample analysis, the LOCEAN (Laboratoire d'Océanographie et du Climat: Expérimentation et Approches Numériques) update Argo datasets co-localized with ship tracks on a regular basis. Data from a few sailing ships, used as experimental platforms, are also taken into account. The processing flow can be summarized as follows:

- For French Research vessels, the TSG real time data are available on the corresponding GOSUD FTP site. Water sample analysis are provided by Coriolis. The delayed mode processing is performed at Laboratoire de Physique des Océans (LPO) in Brest.
- ORE-SSS merchant ships delayed mode data are processed at the IRD Centres in Nouméa and Brest, then at LEGOS in Toulouse and made available on a FTP site.
- Experimental sailing ships (CANOE project) are provided by Coriolis or sent directly to LPO. Some water samples are available. Delayed mode processing is done at LPO.

Delayed mode processing

The delayed mode quality control on TSG data is performed by the scientists at LPO, IRD Centres and LEGOS using the software TSG-QC (http://www.ird.fr/us191/spip.php?article28) developed by US-IMAGO (IRD). There are two levels of control: quality flags and corrections. The quality flags used follows the Coriolis definition (Table 1). It depends on the quality of the data with respect to the climatology, spikes, noise, etc. Then when needed, the time series are adjusted to fit the external data which can be either the water sample analysis and/or the Argo co-localized data. The TSG dataset so produced are a contribution to the GOSUD project and are available in NetCDF Gosud format (https://svn.mpl.ird.fr/us191/tsgqc/trunk/tsg_doc/CORTSG_format_gosud.pdf). An example of TSG-QC processing is given Figure 1.

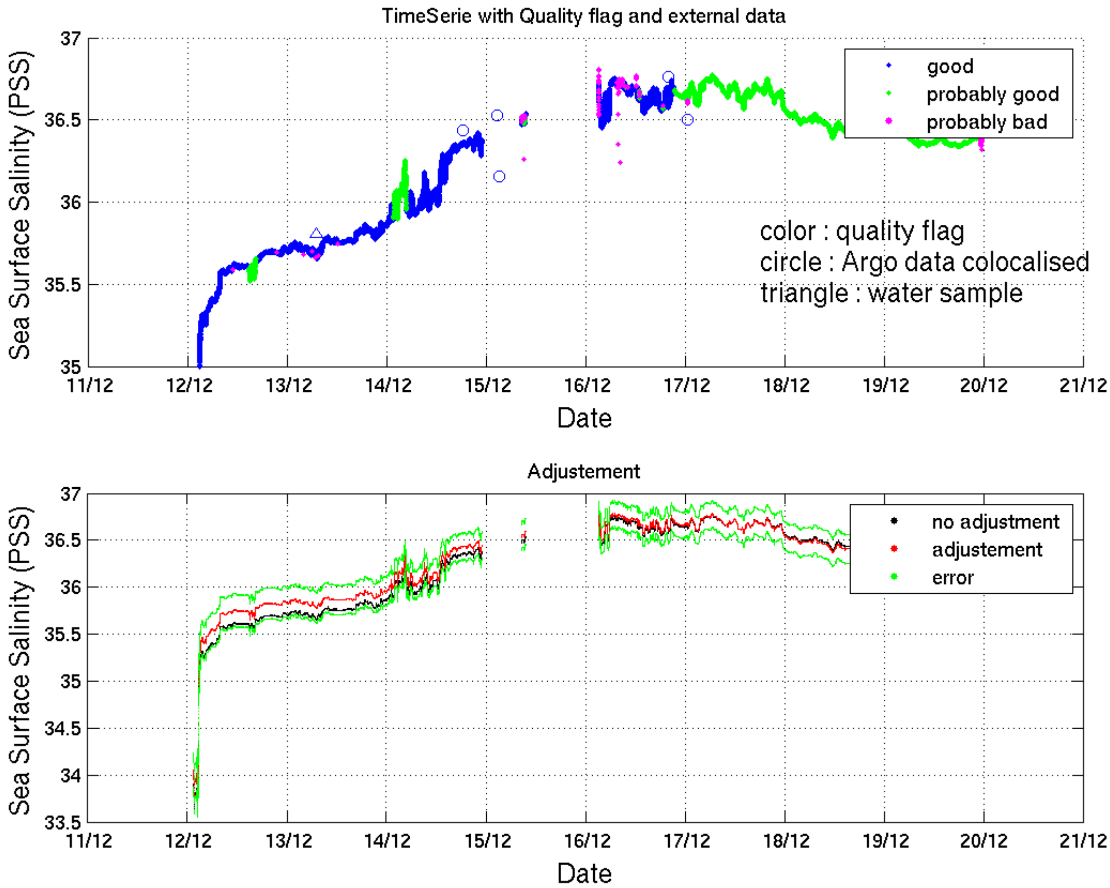

Figure 1: One example of quality control on TSG timeserie. Top panel: timeserie of salinity (PSS 78) with quality flags (color) and external data (salinity from Argo colocalised (circle) and Water Sample (triangle)). Only good quality external data are shown. Bottom panel : Adjusment of timeserie to good quality external data. Timeserie before adjustment (black), timeserie adjusted (red), error on adjustment (green).

We perform the delayed mode quality control of the latest TSG data from French research vessels every month, and back to the past at every water samples delivery. Up to now, we have controlled data from 2007 to 2010. Data from 2008 have not been processed yet because of duplicate data from some well identified French research vessels that are presently under correction at Coriolis.

The processing state for the three years 2007, 2009 and 2010 is summarized Figure 2. Because of the SMOS cal/val requirements, priority has been given to the years 2009 and 2010. Some water samples are still missing in 2010. They should be available soon. This dataset is then merged with the ORE-SSS delayed mode data. The dataset available at the time of this analysis for the years 2007 to 2010 is mapped Figure 3.

Objective Analysis

All these data are then merged to produce gridded fields of temperature and salinity using optimal estimation. This final process constitutes an additional control in the sense that it allows to check with a single processing the consistency of simultaneous datasets and the agreement with climatology. ISAS (In Situ Analysis System, http://wwz.ifremer.fr/lpo/SO-Argo-France/Data-and-products/Global-Ocean-T-S/ISAS-Tool) has been developed by Gaillard et al. (2009b), as a tool to produce these gridded fields from objective analysis of in-situ data coming from multiple sources.

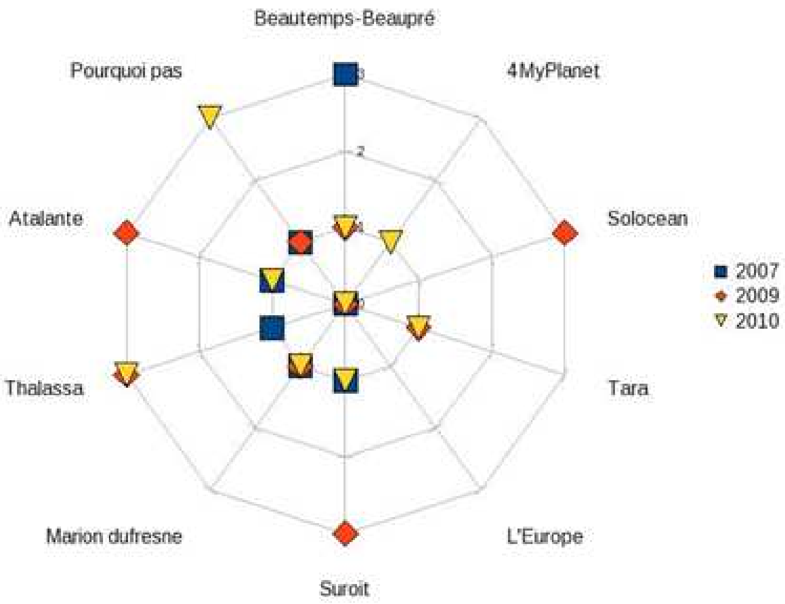

Figure 2: Status of the quality control displayed by ship and year. Level 0: quality flags only (climatology, spikes, noise, sensor behaviour); level 1: adjustment to Argo colocalization only; level 2: adjustment to water samples only; level 4: adjustment to colocalization Argo and water samples.

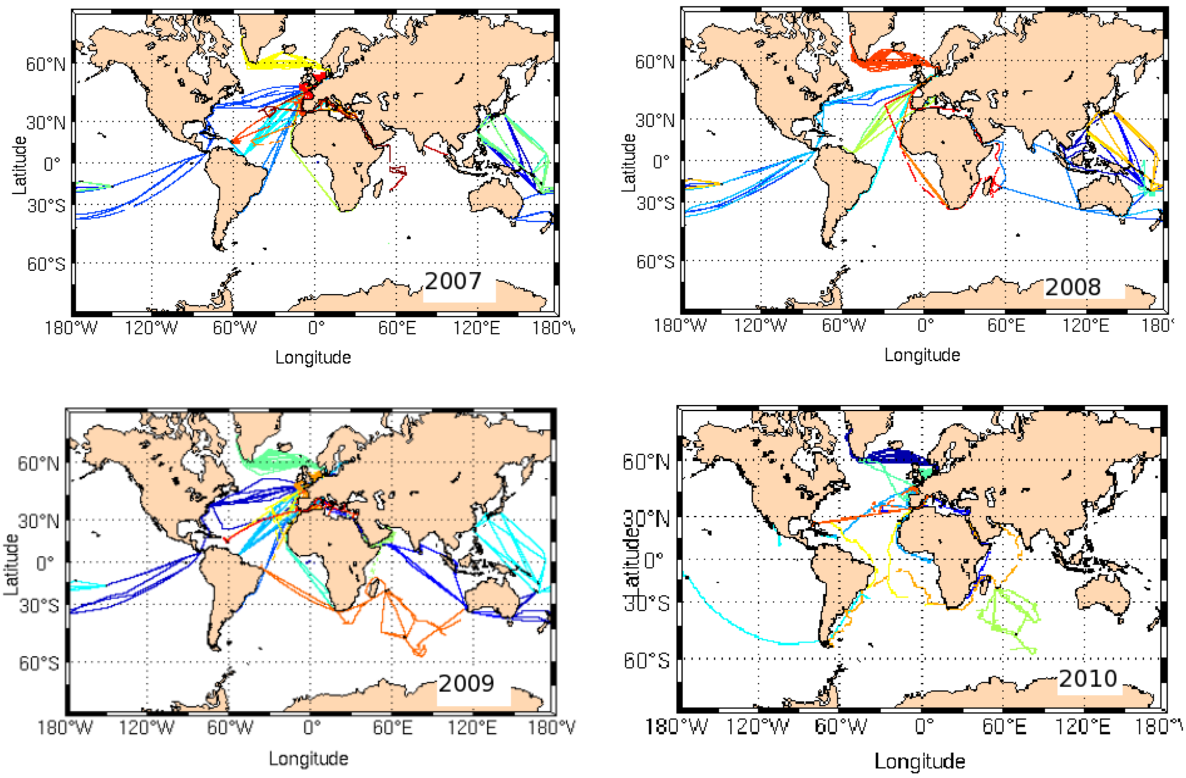

Figure 3: TSG coverage from 2007 to 2010.

The ISAS tool V6.beta

In the context of SMOS cal/val, the objective is to provide and extended and validated in-situ dataset and the corresponding gridded fields at the sea surface. As ISAS has not been specifically developed for the surface, a preliminary work was required to adapt it to this need.

The work started from ISAS V5.3. The ISAS grid covers the globe from 80°S to 90°N with 1/2° Mercator resolution, on 151 standard depth levels between 0 and 2000m. A priori statistics are needed for the analysis: they were obtained from a previous analysis of the period 2002-2008 (von Schuckmann et al. 2009), providing the following reference fields:

- a mean seasonal cycle, or climatology, of temperature and salinity representative of the period
- the corresponding variances (deviation between profiles and monthly mean field) (see Figure 4).
- spatial scales deduced from the Rossby radius of the annual climatology (see Figure 4).

These reference fields and statistics are also used by ISAS for preliminary controls on the dataset and by the CATDS (Centre Aval de Traitement et des Données SMOS) for the real time validation of SMOS data.

The main change with respect to the initial version was to adapt the ISAS-STD pre-processing module to consider specifically the surface layer (levels extending from 0 to 20 meters). For profile data, the surface layer is assumed perfectly mixed above the level of the last measurement, which is then repeated up to the surface. For TSG data, the level sampled by the instrument is assumed to represent the whole surface layer and is repeated over this layer. Most of the time the thermosalinographs measure temperature and salinity at levels varying between 3m and 15m, depending on the vessels and their draught. The error associated with extrapolated data is increased proportionally to the distance from the measurement level. A second processing is applied to the data before producing the final ‘STD’ (standardized) files to be used by ISAS. Data from the same platform obtained within a given time and space window are averaged to reduce the oversampling that may induce matrices ill conditioning. This processing is particularly efficient on the high frequency sampled TSG data.

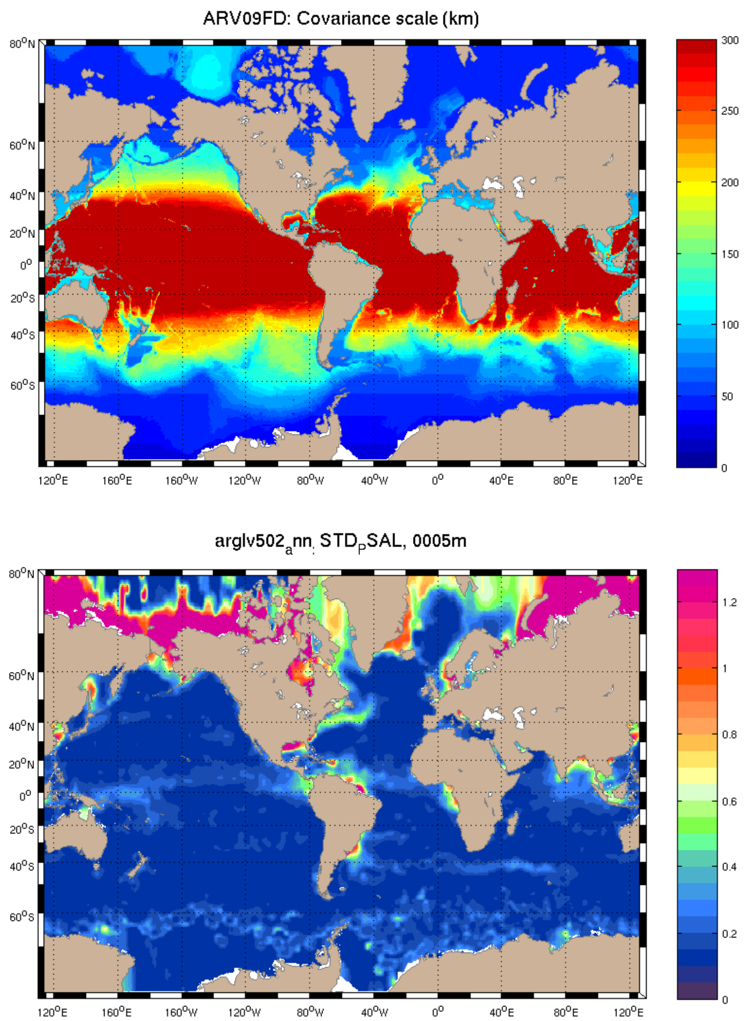

Figure 4: Top panel: Covariance scales. Bottom panel: a priori variance of salinity (PSS 78).

Near Real Time Analysis in support of SMOS

Until now, TSG have not been used in ISAS analysis because quality control procedures were still under development. They are now operational. In this first attempt of including TSG data, we can evaluate their relative weight in the global dataset by first examining the number of data. In the case of June 2010 analysis (Figure 5), we note that TSG data represent 49% of the total amount of raw data. This ratio decreases to less than 6% in the pre-processed STD data because of the high frequency sampling rate that lead to a lot of averaging. This has to be compared with the Argo data ratio that rises from 13% to 67%.

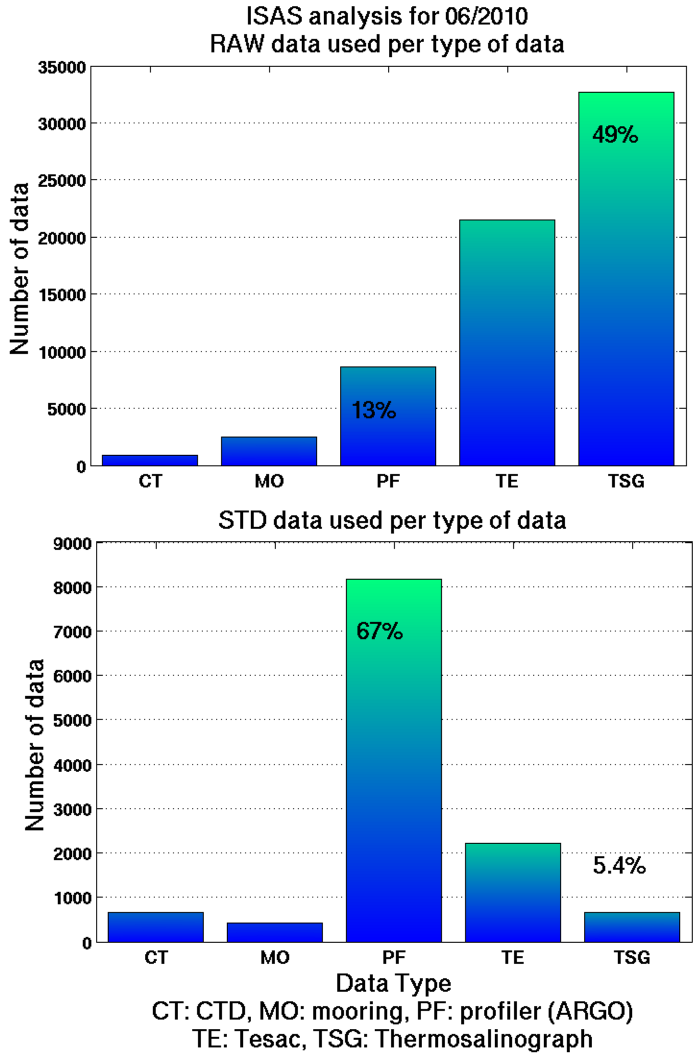

Figure 5: Number of in-situ data used to process the objective analysis of 06/2010, according to their source: TE for low resolution data from GTS (Global Telecommunication System), CT for CTD, MO for Mooring, PF for Profiler and TSG). Top panel: raw data. Bottom panel: pre-processed data.

However, it should be noted that if Argo is a global dataset, at present time our TSG database is mainly fed by French laboratories and thus is far from being global. A strong potential exists for increasing this database by developing new platforms (CANOE project) and through international collaboration within GOSUD. Nevertheless, preliminary results show that even with a limited TSG dataset, including this data improves the final analysis (Figure 6). The analysis integrating TSG (Figure 7) are now validated and ready to be performed in operational mode.

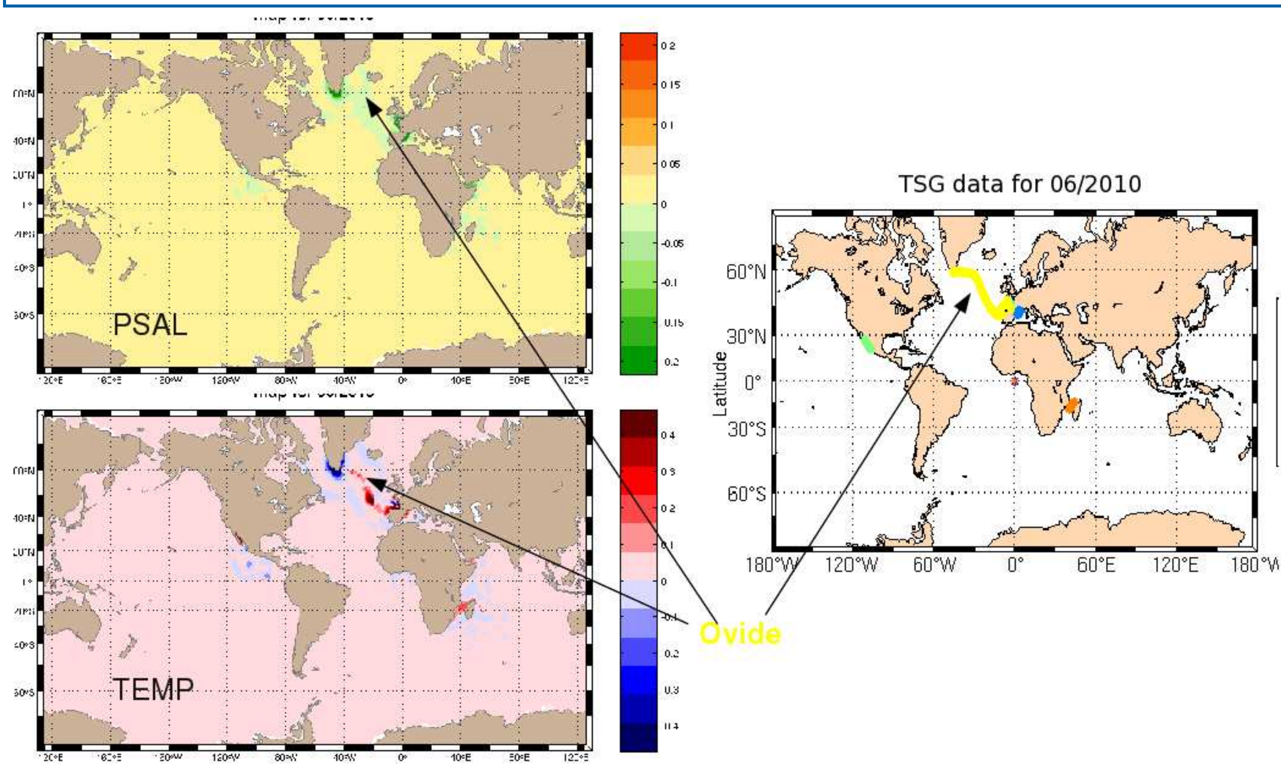

Figure 6: Impact of TSG data on the analysis at 5m depth for 06/2010 with and without TSG data included in the dataset. Left panel: map of the difference in salinity and temperature. Right panel: TSG data available for 06/2010. Arrows indicate the track of the TSG for the Ovide cruise.

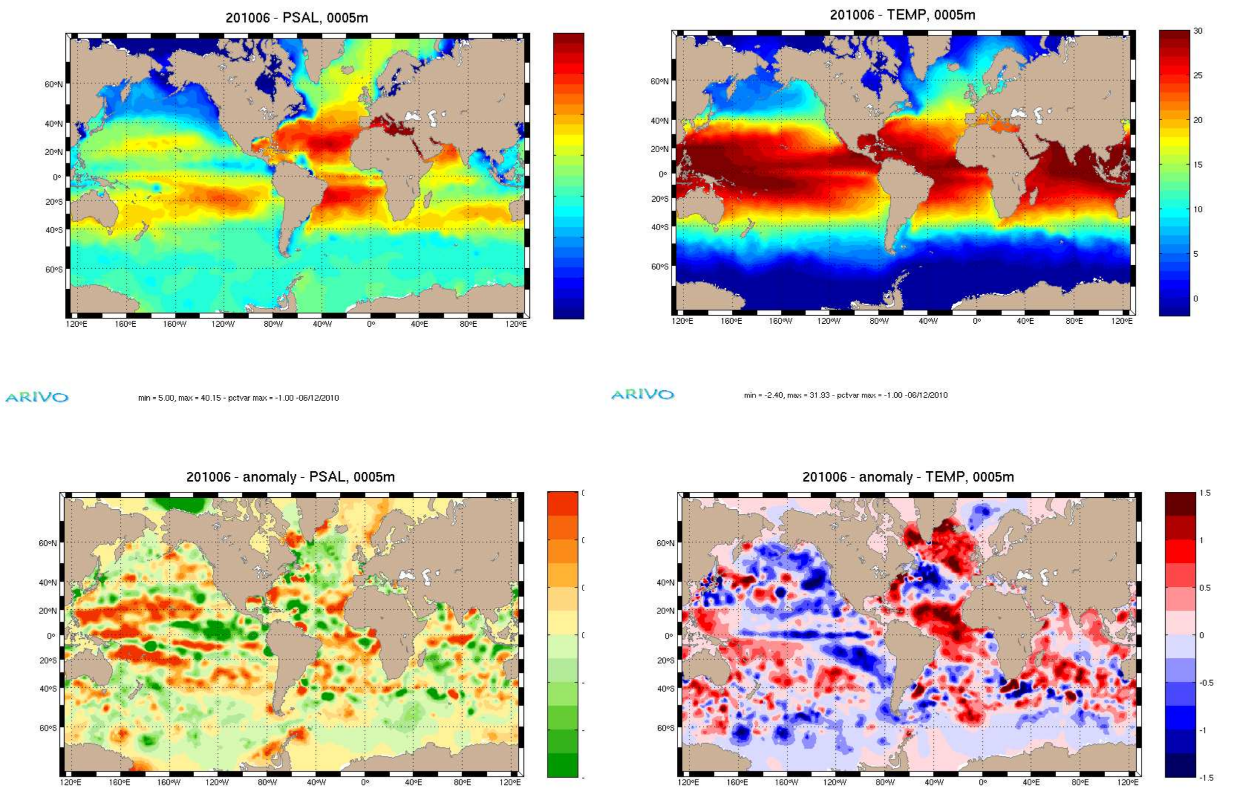

Figure 7: Analysed fields of 06/2010 at 5m depth, with TSG included in the dataset. From top left to bottom right: salinity (PSS 78) and temperature (℃), corresponding anomaly of salini ty and temperature.

Conclusion

In the context of SMOS cal/val, our goal is to provide monthly gridded fields of SSS and SST and the corresponding dataset in near real time and to take into account as many validated observations as possible. It appears from the first results that ISAS tool, extended to process surface dedicated measurements, is well adapted to this goal. We are now able to produce gridded fields and datasets based on Coriolis data and TSG that are delivered to the CATDS cal/val team each month. Our products have already been used to evaluate the real time SMOS data and to detect biases in order to improve the algorithms (Yin et al. 2010 and Reul et al. 2010).

The next step will be to increase the surface database. We will focus on qualified data only. Different sources can be considered. The first one is the drifting buoys equipped with conductivity sensors from LOCEAN database. They are validated and easily accessible. Regarding TSG data, until now French data only have been processed. International contributions within GOSUD program have now to be considered. Besides, new platforms presently under development can be taken into account.

Acknowledgments

For this work, E Brion was supported by CNES grant OT5-2630. Thanks to J. Grelet and Y. Gouriou, from IRD-US-IMAGO for providing and maintaining the TSG-QC software. Thanks to Nicolas Martin from LOCEAN for providing the Argo datasets co-localized with TSG tracks.

References

Coatanoan C. and Petit De La Villeon L., 2005. Coriolis report 04-047.
(http://www.coriolis.eu.org/content/download/4918/36060/file/cordo-rap-04-047-quality-control.pdf).

Gaillard F., E. Autret, V.Thierry, P. Galaup, C. Coatanoan, and T. Loubrieu, 2009b. Quality control of large Argo data sets. *Journal of Atmostpheric and Oceanic Technology*, 26(2), 337–351.

Gaillard F., E. Brion, R. Charraudeau, 2009a, ISAS – V5: Description of the method and user maual. Rapport LPO 09-04.

Reul Nicolas, Brachet Sidonie, Tenerelli Joseph, Chapron Bertrand, Tournadre Jean, Vandemark Doug, 2010. Tropical Ocean Major Freshwater Pools Characteristics as Viewed from Space with Low Frequency Microwave Radiometers, Oral presentation, ESA-Living Planet Symposium, Bergen, 28 june to 2 july 2010.

Reverdin G., F. Gaillard, S. Contardo, D. Mathias, Y. Gouriou, D. Dagorne, 2006. Qualification des mesures navire: salinité de surface. Rapport Coriolis cordo-07-023, 68pp. Octobre 2006

von Schuckmann K., F. Gaillard and P.-Y. Le Traon, 2009. Global hydrographic variability patterns during 2003-2008, J. Geophys. Res., 114, C09007, doi:10.1029/2008JC005237.

Yin Xiaobin, Boutin Jacqueline, Meirold-Mauntner Ingo, Vergely Jean-Luc, Waldteufel Philippe, Spurgeon Paul, 2010, Preliminary results of SMOS Data Analysis over the Ocean During the Commissioning Phase, Oral presentation, ESA-Living Planet Symposium, Bergen, 28 june to 2 july 2010.

How should the Argo array be extended to better monitor the Global Ocean heat content variability?

By Mélanie Juza[1], Thierry Penduff[1,2], Bernard Barnier[1]

[1]Laboratoire des Ecoulements Géophysiques et Industriels, Grenoble, France
[2]Earth, Ocean and Atmospheric Science Department, The Florida State University, Tallahassee, Florida, USA

Abstract

The global Argo array of profiling floats is used to monitor the Global Ocean heat content (OHC) variability, but areas shallower than 400m, ice-covered regions, and the waters located below 2000m remain almost (or fully) inaccessible. A ¼° global ocean/sea-ice simulation is used to determine how these three unobserved areas, which represent 51.5% of the whole ocean volume, contribute to the seasonal and interannual global OHC variability. Although partial, the observed ocean volume gives a very accurate estimate of globally-integrated OHC variability in terms of phase. However, in terms of amplitude, Argo floats are presently exploring a body of water where the integrated OHC amplitude is 13% larger than its global simulated counterpart at seasonal timescales, and 5% smaller at interannual timescales. Our results suggest that these biases could be divided by 2-3 by complementing Argo data by shallow-water profiles; extending the array below 2000m or below sea-ice may reduce these biases too, but less markedly.

Introduction and motivations

The ocean heat content (OHC) plays a primary role in the Earth's heat balance (Levitus et al., 2001). The Argo array of profiling floats (Roemmich et al., 2004) has been collecting temperature and salinity profiles over most of World Ocean for the last decade. More than 3000 active floats are currently drifting throughout the global ocean, helping monitor the ocean variability and the climate evolution by analysing some relevant quantities, such as the global OHC in the upper 2000m. Such observations and Ocean General Circulation Models are being used to study the variability of the upper OHC (Levitus et al., 2005, Lyman et al., 2006, AchutaRao et al., 2006, 2007). Most of these estimates are limited to the upper 750m (Willis et al., 2004) which is the maximum depth of XBT profiles, and at most to the upper 3000m (Levitus et al., 2005) since historical CTD data are very sparse at greater depths.

Over the last 10 years, Argo data have strongly increased the number of hydrographic profiles available globally, but three main regions still remain beyond reach. First, the body of water sitting below 2000m remains unsampled by Argo although it accounts for 48% of the Global Ocean volume, continuously interacts with the upper layers through advective and mixing processes, significantly contributes to the global energy balance (Levitus et al., 2005, Johnson et al., 2007), and could add 2-10% to the trend of the global ocean heat content (Johnson et al., 2007). Second, most Argo floats are unable to transmit hydrographic data when sea-ice is present (Arctic and Southern Oceans in particular). Finally, most profiling floats do not properly sample relatively shallow areas because their nominal parking depth is 1000m. In other words, the contributions of deep layers, ice-covered regions, and relatively shallow areas to the variations of the global OHC remain difficult to assess from Argo data, and poorly known in the former two zones.

In this study, we use a global ocean simulation to estimate and compare the variabilities of heat content in the simulated Global Ocean, in the volume that is accessible to Argo floats (i.e. the “Argo ocean” where shallow waters, deep layers and ice-covered regions are ignored), and in each of these unobserved regions, at seasonal and interannual timescales. These results are then used to identify the area(s) where the observational array may be extended for a more accurate monitoring of the global OHC variability. Note that the impact of the actual array's irregular geometry on the estimation of OHC fluctuations in the “Argo ocean” is not our focus here; these results will be reported elsewhere.

The geographical restrictions of the Argo array and our methodology are presented in Section 2. Section 3 presents the global OHC (detrended) variabilities derived from the simulation at seasonal and interannual timescales, which we will consider as the “truth”. The biases induced by the Argo restrictions on OHC anomalies will then be investigated in terms of phase and amplitude, and we will attempt to determine where the observational array could be extended to improve the estimation of the global OHC variabilities. Conclusions are given in Section 4.

Datasets and methodology

Geographical restrictions of the Argo array

Figure 1 shows the annually-averaged number of valid Argo profiles available globally within 3° by 3° boxes over the period 2000-2006 (Argo locations are taken from ENACT-ENSEMBLES database, Ingleby and Huddleston, 2007). This panel shows the uneven coverage of Argo profiles over the global ocean: the mid-latitude northern hemisphere (in particular the North Atlantic, Northwest Pacific, North Indian Ocean, and the Eastern Mediterranean Sea) is much better sampled than high-latitude regions (Southern and Arctic oceans) and relatively shallow basins (e.g. Indonesian Seas, North Sea).

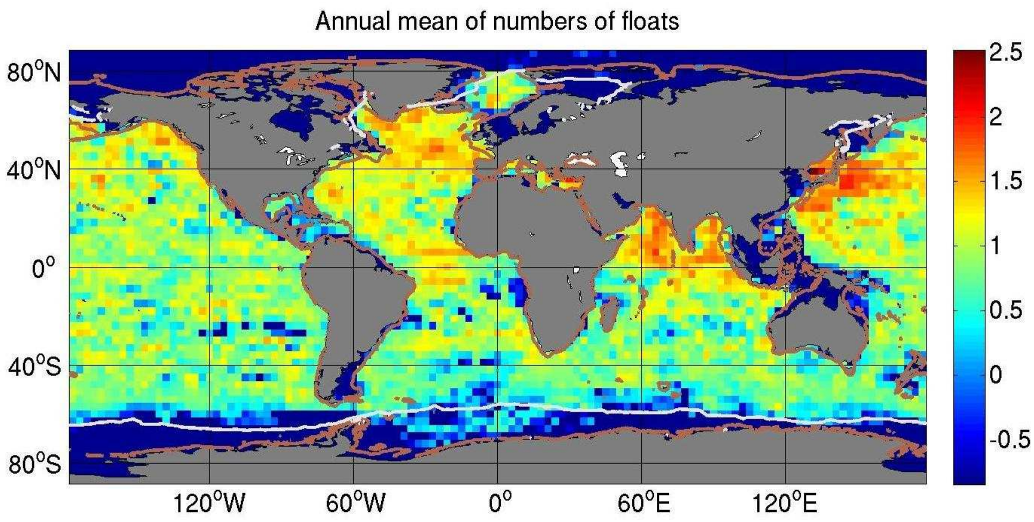

Figure 1: Annual mean of number of Argo profiles available over 2000-2006 in 3°x3° boxes (log scale). The 20% mean sea-ice concentration limit and the isobath 400m are shown as white and brown lines, respectively.

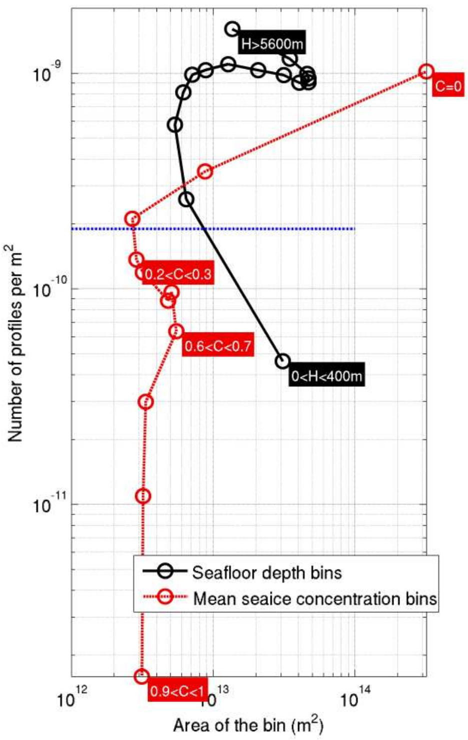

Figure 2: Number of Argo profiles per unit area (i.e. density of profiles, ordinate) within bins of seafloor depth H (black circles, successive 400m-wide bins), and within bins of mean sea-ice concentration C (red circles, successive 0.1-wide bins). The abscissa indicates the area (m2) corresponding to each bin. The density of profiles is similarly small below the blue line, i.e. in areas shallower than 400m and where the mean sea-ice concentration exceeds 0.2.

Figure 2 shows the density of Argo profiles within bins of seafloor depth (black circles) and within bins of mean sea-ice concentration (red circles) over 2000-2006. This reveals that areas shallower than 400m, and that regions where the mean sea-ice concentration exceeds 20% over the period are similarly and strongly undersampled. We will therefore consider that ice-covered regions are those where the sea-ice concentration averaged over 2000-2006 in our simulation exceeds 20%; these regions are located poleward of the white lines in Figure 1 and account for 8.6% of the global ocean surface (5.5% of its global volume). We will define shallow water areas such as regions where the seafloor depths are shallower than 400m (brown contours in Figure 1) in the free-ice ocean (where mean sea-ice concentration < 20%); they represent 6% of the global ocean surface and 0.2% of its volume. We investigate below the contributions in the global OHC variability of these two poorly observed regions, of the unobserved waters located below 2000m (whose volume represents 45.8% of the free-ice ocean), and of the "Argo ocean".

Global model simulation

We make use of the so-called ORCA025-G70fo eddy-admitting global ocean/sea-ice simulation performed by the DRAKKAR Group (2007) [http://www.drakkar-ocean.eu]. The model configuration is based on the NEMO code (Nucleus for European Models of the Ocean, Madec, 2008). The model grid has 46 vertical levels, and a ¼° horizontal resolution. Thi s global simulation is driven without data assimilation by a realistic daily interannual forcing between 1958 and 2007 (DFS3 forcing, Brodeau et al., 2010). This model configuration and simulation results are described in detail and evaluated in e.g. Barnier et al. (2006), Penduff et al. (2007, 2010). Simulated three-dimensional temperature fields are archived as successive 5-day means from which monthly means are derived.

The 2000-2006 time series of monthly temperature fields at each gridpoint are first linearly detrended, for 2 main reasons: [1] linear trends may be due to low-frequency fluctuations that are not properly resolved in relatively short (observed or simulated) time series; [2] simulated trends may differ from observed because model stratifications need decades to adjust (in particular below the thermocline). Removing linear trends is therefore a consistent way to limit the possible impact of model discrepancies, and to focus our investigation on the (interannual) scales which are properly resolved in our 7-year dataset.

Global ocean heat content anomalies

Detrended time series of three-dimensional monthly temperature are used to compute the mean 3D temperature field ($\overline{T}$) over the period 2000-2006, the 3D monthly climatological temperatures (Tm, m ϵ [1,12]) over the same period, and the series of annually-averaged 3D temperature field (Ta, a ϵ [2000,2006]). The series of monthly heat content anomalies OHCAm are then computed over various domains (V) as in Antonov et al. (2004); the (detrended) series of monthly (m) and annual (a) heat content anomalies OHCAm,a are defined in a similar way (equation 1):

$$OHCA_{m,a} = \rho_0 Cp \iiint_V (T_{m,a} - \overline{T}).dV \quad (1)$$

where ρ0 = 1020kg.m-3 is the seawater density, Cp = 4000J/kg/°C denotes the specific heat capacity of seawate r at constant pressure. Integration domains D may denote either the whole global ocean (yielding the "true" simulated OHCA), the deep, shallow, or ice-covered regions (yielding OHCAs that are inaccessible to Argo), the "Argo ocean", or the latter extended to one of the three unobserved regions.

OHCAm and OHCAa time series calculated over the observed or extended domains are then compared to the globally-integrated ("true") reference (G) in terms of phase (correlation between OHCA and OHCAG) and amplitude (std(OHCA)/std(OHCAG)).

Observable, non-observed and extended OHC variabilities

Figure 3 shows the time series of detrended monthly (top panel) and annual (bottom panel) ocean heat content anomalies (OHCAm and OHCAa, respectively) over the whole ("true") and observable oceans, at global scale and in the northern and southern hemispheres separately.

"True" OHC variabilities

As expected, the "true" OHCAm exhibits opposite seasonal phases in the northern and southern hemispheres (Figure 3, upper panel, solid lines). The phase of the global OHCAm follows the phase of its southern component which accounts for a greater volume. Total OHCAm reaches its maximum in April (0.3×10^{23}J) and its minimum in August (-0.25×10^{23}J). The interannual OHCAa time serie exhibits a smaller, yet substantial, variability: its global value increases by more than 0.5×10^{22}J from 2000 to 2001, decreases until 2003 to -0.4×10^{22}J, and increases again from 2003 to 2006. The interannual variability of the global OHCAa also appears to be more constrained by its southern component.

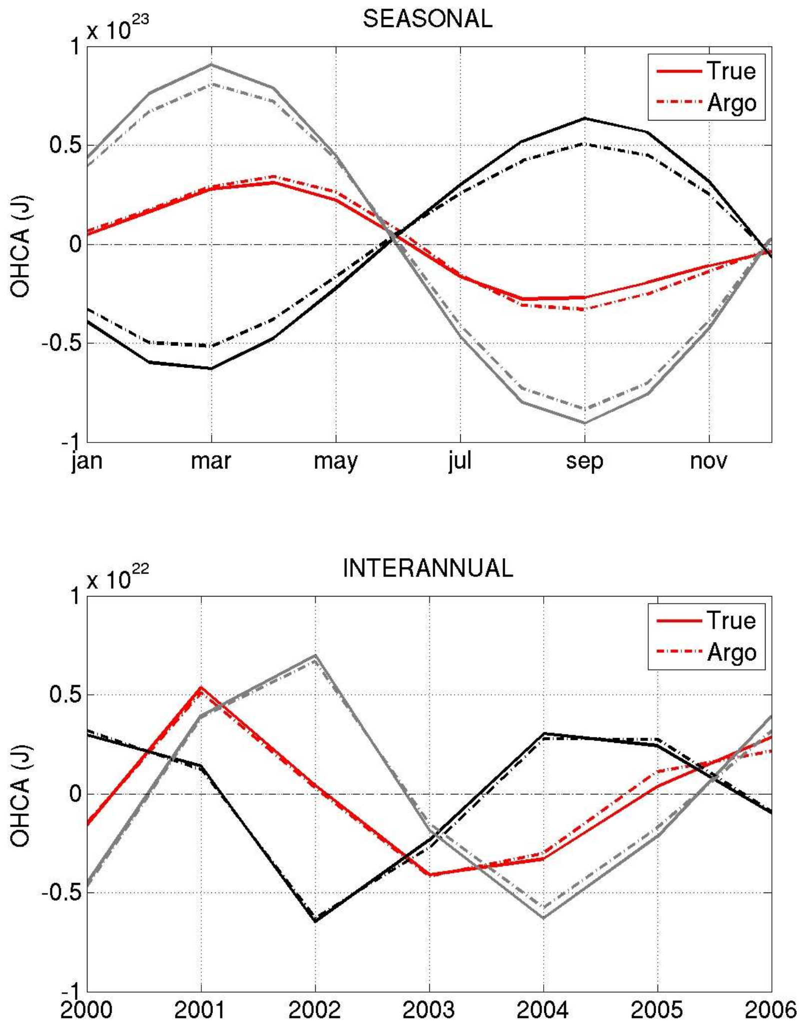

Figure 3: Detrended monthly (top panel) and annual (bottom panel) heat content anomalies (J) estimated from the whole ("true") ocean (solid line) and the observable (by Argo) ocean (dash-dotted lines). Results are shown for the global ocean (red lines), for the northern (black lines) and southern (grey lines) hemispheres.

Comparison with observable OHC variability

The seasonal and interannual OHCA variabilities that are accessible to the Argo array (i.e. within the "Argo ocean") are shown as dash-dotted lines in Figure 3. Their time series are extremely well correlated with the "true" OHCA at both timescales (Figure 4, left panels). However, Argo's geographical restrictions lead to amplitude biases (Figure 4, right panels): the amplitude of the observable OHC seasonal variability is substantially (13%) larger than the "true" OHC variability. The Argo sampling, indeed, yields an underestimation of seasonal OHC amplitudes in the northern and southern hemispheres (about -19% and -9%, respectively); this north-south contrast results in overestimated OHCA amplitude at global scale because the southern hemisphere contributes more to the global integral. At interannual timescale, the observable OHC variability is smaller (by around 5%) than its global counterpart. This is also mostly due to geographical restrictions in the southern hemisphere (7%).

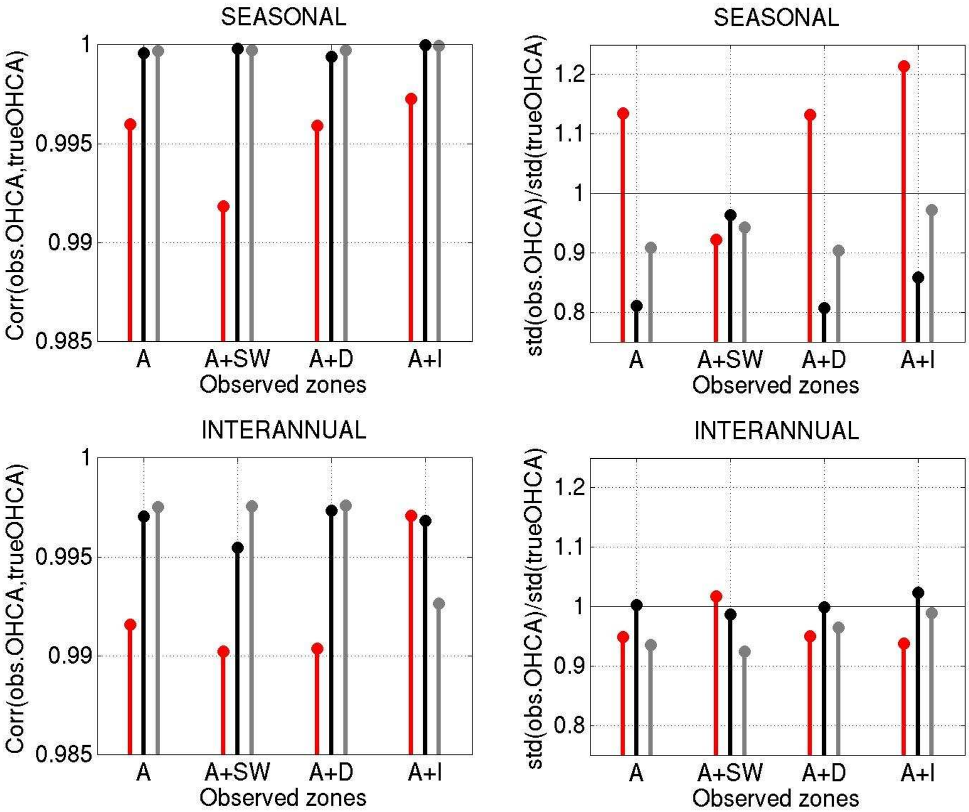

Figure 4: Correlations (left panels) and amplitude ratios (right panels) between OHC time series integrated over various subregions (i.e. A, A+SW, A+D, A+I, see text), and the globally-integrated "truth". Results are shown at global scale (red), in the northern (black) and southern (grey) hemispheres, both at seasonal (top panels) and interannual (bottom panels) timescales.

Unobserved OHC variability

We are now considering OHC variabilities over the shallow waters (SW), the deep ocean (D) and the ice-covered regions (I) which are not (or poorly) sampled by the Argo array (Figure 5). They are all about 10 times smaller than in the "Argo ocean" at both timescales (except the seasonal variability of the deep ocean which is more than 100 times smaller) for different reasons. Although the specific OHC seasonal variability (variability per unit volume) is larger in the SW zone than in the "Argo ocean" because the latter extends much deeper than large seasonal variabilities do, the SW volume is much smaller hence yielding a smaller integrated variability. In contrast, the deep and ice-covered regions include much larger volumes than shallow waters but specific OHC variabilities are small there hence yielding relatively small integrated contributions. Phase relationships between the unobserved zones and the observed region differ in more complex ways. For instance, the anticorrelation seen between seasonal OHC variabilities in the Argo and SW zones comes from the presence of more shallow waters in the northern hemisphere, and more regions accessible to Argo in the southern hemisphere. Despite this geographical asymmetry, the phases of SW and "Argo" OHC's variabilities are in good agreement at interannual timescales, probably because northern and southern interannual variabilities are not expected to be particularly anticorrelated.

The small amplitudes of "unobserved" OHCs suggest that the phase and amplitude of OHC variabilities integrated over the "Argo ocean" extended to one of the three other zones may not dramatically differ from their "Argo" counterparts. However, the non-negligible amplitudes of unobserved OHC variabilities, and their diverse phase relationships with presently observable variabilities might possibly lead to sizeable changes in the accuracy of Argo-derived OHC variability estimates as the array is (virtually) extended to such regions. This is investigated in the next section.

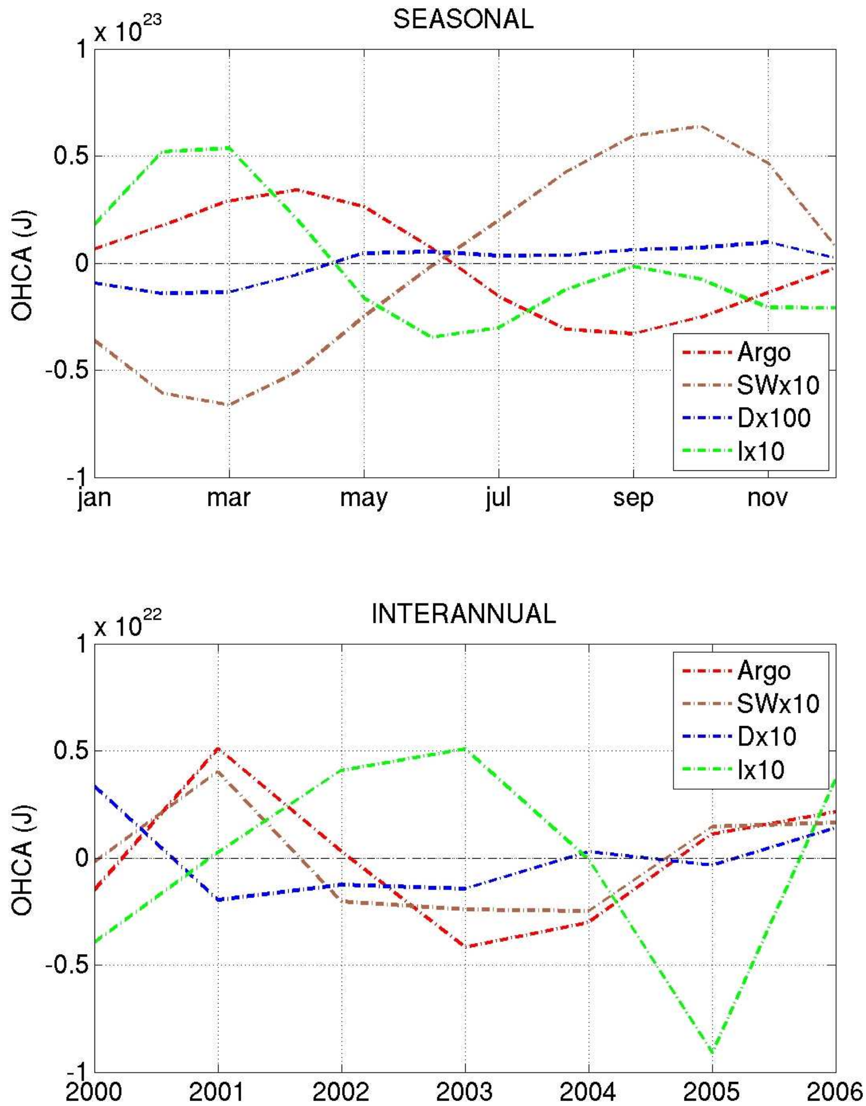

Figure 5: Detrended monthly (top panel) and annual (bottom panel) heat content anomalies (J) estimated from the "Argo ocean" (red), the Shallow Water areas (SW, in brown), the Deep ocean (D, in blue) and Ice-covered regions (I, in green) at global scale. The heat content anomalies of the unobserved regions have been multiplied by a factor (indicated in the legends) for clarity.

Potential benefits of three geographical extensions on Argo's OHC variability estimates

We now compare "true" OHC variabilities with those computed over the presently observable Argo "A" region, and over the "A" region successively extended to each unobserved region (shallow water areas A+SW, deep ocean A+D, and ice-covered regions A+I). The left panels in Figure 4 reveal that, as mentioned earlier, the temporal correlations between "true" and "A" OHCs are extremely high, i.e. larger than 0.99, at both seasonal and interannual timescales. Extending the sampling to any of the three unobserved regions does not affect this excellent agreement: provided that the distribution of temperature profiles is dense and regular enough over accessible regions (an issue not addressed here but that should be kept in mind), extending the array may not improve the phase of the estimated global OHC variability (which is already extremely well correlated to the "truth").

However, our results show that the amplitudes of partially-sampled OHC variabilities may be more affected by geographical extensions. The right panels in Figure 4 suggest that extending the presently observable area to either deep layers (A+D) or ice-covered regions (A+I) would not compensate for the O(10%) overestimation of the "A" OHC seasonal cycle, or for the 5% underestimation of the "A" OHC interannual variability. However, the extension of the observable region to shallow waters (A+SW) may substantially decrease both biases: both would be reduced in absolute value by a factor of 2 (seasonal cycle) or 3 (interannual variability).

At seasonal timescales (Figure 4, upper right panel), it is interesting to note that including shallow waters yields the clearest decrease of the seasonal OHC amplitude bias in the northern hemisphere (black line) where most shallow waters are found indeed. In other words, the 13% overestimation of the seasonal OHC cycle when only the “A” region is considered is partly compensated for by including shallow waters, whose seasonal OHC cycle is opposite to the “A” cycle because they are mostly found in the northern hemisphere (see Figure 4, top panel).

The estimated amplitude of the interannual OHC variability may be improved as well by including shallow waters to the “Argo” ocean (A+SW), although the individual amplitudes of northern and southern interannual cycles would be slightly degraded (Figure 4, bottom right panel). This is again a consequence of peculiar cross-correlations between OHCs within various subregions.

We have finally evaluated (not shown) the relative benefits of including to the Argo zone two regions out of the three considered here (i.e. A+SW+I, A+D+I, and A+SW+D). These results show that given OHC variances and cross-correlations between OHCs within all areas, the joint extension of the “A” region to both shallow waters and ice-covered regions would decrease to less than 3% the seasonal and interannual OHC amplitude biases in both hemispheres and in the global ocean simultaneously. In any case, not including shallow waters (i.e. A+D+I) would result in smaller amplitude bias reduction.

Conclusion

Three main regions remain inaccessible to the existing Argo array of profiling floats: the layer located below 2000m, regions shallower than 400m, and ice-covered regions. We diagnosed from a recent, multidecadal global eddy-permitting simulation the seasonal and interannual variabilities of the ocean heat content (OHC) over the volume “A” accessible to Argo, over the three unobserved regions individually and over volumes including “A” extended to each region. Our main results are summarized below:

The amplitude of the OHC variability over region A is about 13% larger (resp. 5% smaller) than the actual global variability, at seasonal (resp. interannual) timescales.

OHC variabilities integrated over the three (as yet) inaccessible regions are much smaller than over the A volume, but their phases are very different: virtually extending the “observed” ocean toward either three regions can therefore improve or deteriorate the estimation of global OHC fluctuations.

Extending the accessible volume to shallow waters may be most beneficial for the estimation of global OHC variabilities at both seasonal and interannual timescales.

Extending the accessible volume below 2000m or toward ice-covered regions instead may improve the estimation of OHC fluctuations in each hemisphere at seasonal and interannual timescales, but yield a stronger global bias.

Our results demonstrate that Argo floats drift where most of the seasonal and interannual OHC variabilities are found. The Argo dataset is therefore clearly vital for climate monitoring, although complementing it with shallow-water profiles (captured by Argo or by other means) could improve the accuracies of globally-integrated estimates.

It would be interesting to quantify how the sparsity of the actual, dispersed, array affects the biases that we report in volume A. Ensembles of accurate, long-term simulations with realistic thermal trends (that may not be available yet) could also be analysed as proposed here to assess in-situ estimates of (natural and/or anthropogenic) oceanic warming. Such studies are left for the future.

References

AchutaRao, K.M., B.D. Santer, P.J. Gleckler, K.E. Taylor, D.W. Pierce, T.P. Barnett, and T.M.L. Wigley (2006), Variability of Ocean Heat Uptake: Reconciling Observations and Models, Journal Geophysical Research, 111, C5, C05019, doi: 10.1029/2005JC003136.

AchutaRao K.M., M. Ishii, B.D. Santer, P.J. Gleckler, K.E. Taylor, T.P. Barnett, D.W. Pierce, R.J. Stouffer, and T.M.L. Wigley (2007), Simulated and observed variability in ocean temperature and heat content, Proceedings of the National Academy of Sciences, 104, doi: 10.1073/pnas.0611373104.

Antonov, J. I., S. Levitus and T. P. Boyer (2004), Climatological annual cycle of ocean heat content, Geophysical Research Letters, vol. 31, L04304, doi: 10.1029/2003GLO18851.

Barnier, B., G. Madec, T. Penduff, J.-M. Molines, A.-M. Treguier, J. Le Sommer, A. Beckmann, A. Biastoch, C. Böning, J. Dengg, C. Derval, E. Durand, S. Gulev, E. Remy, C. Talandier, S. Theetten, M. Maltrud, J. McClean, B. De Cuevas (2006), Impact of partial steps and momentum advection schemes in a global circulation model at eddy permitting resolution, Ocean Dynamics, 56(5-6), 543-567, doi: 10.1007/s10236-006-0082-1.

Brodeau, L., B. Barnier, T. Penduff, A.-M. Treguier, and S. Gulev (2010), An ERA-40 based atmospheric forcing for global ocean circulation models, Ocean Modelling, 31, 3-4, 88-104.

DRAKKAR Group (2007), Eddy-permitting ocean circulation hindcasts of past decades, Clivar Exchanges, 42, vol. 12, No 3, 8-10.

Ingleby, B., and M. Huddleston (2007), Quality control of ocean temperature and salinity profiles - historical and real-time data, Journal of Marine Systems, 65, 158-175, doi: 10.1016/j.jmarsys.2005.11.019.

Johnson, G.C., S. Mecking, B.M. Sloyan and S.E. Wijffels (2007), Recent Bottom Water Warming in the Pacific Ocean, Journal of Climate, 20, 5365-5375, doi: 10.1175/2007JCLI1879.1.

Levitus, S., J. L. Antonov, J. Wang, T. L. Delworth, K. W. Dixon, A. J. Broccoli (2001), Anthropogenic Warming of Earth's Climate System, Science, vol. 292. no. 5515, pp. 267-270, doi: 10.1126/science.1058154.

Levitus, S., J. Antonov, and T. Boyer (2005), Warming of the world ocean, 1955-2003, Geophysical Research Letters, 32, L02604, doi: 10.1029/2004GL021592.

Lyman, J. M., J. K. Willis, G. C. Johnson (2006), Recent cooling in the upper ocean, Geophysical Research Letters, 33, L18604, doi: 10.1029/2006GL027033.

Madec, G. (2008), NEMO reference manual, ocean dynamics component: NEMO-OPA. Preliminary version, Tech. Rep. 27, Notes du Pôle de modélisation, Institut Pierre-Simon Laplace (IPSL), France, iSSN No 1288-1619.

Penduff, T., J. Le Sommer, B. Barnier, A.-M. Treguier, J.-M. Molines, and G. Madec (2007), Influence of numerical schemes on current-topography interactions in ¼° global ocean simulations, Ocean Science, 3, 509-524.

Penduff, T., M. Juza, L. Brodeau, G.C. Smith, B. Barnier, J-.M. Molines, A.-M. Treguier and G. Madec (2010), Impact of global ocean model resolution on sea-level variability with emphasis on interannual time scales, Ocean Science, 6, 269-284.

Roemmich, D., S. Riser, R. Davis, and Y. Desaubies (2004), Autonomous profiling floats: workhorse for broad-scale ocean observations, Journal of Marine Technology Society, 38, number1.

Willis, J.K., D. Roemmich, and B. Comuelle (2004), Interannual variability in upper ocean heat content, temperature and thermosteric expansion on global scales, Journal of Geophysical Research, vol. 109, C120306, doi: 10.1029/2003JC002260.

QuO Va Dis? The Mercator Ocean quarterly validation bulletin: recent developments and prospects.

By Marie Drévillon[1], Charly Régnier[1], Charles Desportes[1], Eric Greiner[2], Stéphanie Guinehut[2] and the Mercator Océan R&D team

Contact: qualif@mercator-ocean.fr

[1] Mercator Océan, Ramonville St Agne, France
[2] CLS, Ramonville St Agne, France

Introduction

Since the last issue of this newsletter dedicated to CORIOLIS, Mercator Ocean has issued 3 quality bulletins (April-May-June 2010, July-August-September 2010, October-November-December 2010) names "QuO Va Dis?" Quarterly Ocean Validation Display (see newsletter # 37 "working together" http://www.mercator-ocean.fr/documents/lettre/lettre_37_en.pdf). These bulletins are sent to the GMMC scientific committee and other scientific collaborators of Mercator Ocean. When they will reach a satisfactory format they will be published on the Mercator Ocean website (the objective is the end of 2011). The two aims of the bulletin are to **monitor the quality of the Mercator Ocean products** (and to give a as much as possible synthetic view of this quality) and to **better interact with data centers** (in particular to better organise the feedback of blacklisted observations).

The first objective is partly fulfilled after one year. We now work on obtaining a better synthesis of the results and selecting pertinent quality indicators. The production of the graphics is partly automatic, but is still needed to include the new Mercator Ocean systems (IBI, BIOMER, and new daily forecasts) and to add user oriented information such as lagrangian statistics.

In order to reach the second objective, the new PSY3 and PSY2 systems now include (as well as the GLORYS reanalysis) a quality control of input Temperature and Salinity profiles based on data assimilation innovations. The feedback to CORIOLIS has now to be organised on a regular basis.

This short article first gives a summary of what has been proposed in the QuO Va Dis? Bulletins (first section), and in a second section we shortly describe the work that is in progress including collaborations with CORIOLIS.

The QuO Va Dis contents: main achievements

The main climatic state of the atmosphere, sea ice and SST for the period of interest is first described, together with the status of the systems and input observations. The bulletins then include many comparisons to CORIOLIS data such as data assimilation statistics in predefined regions and CLASS4 comparisons. The CLASS4 metrics (from MERSEA and GODAE) are the collocation of Mercator Ocean daily average products (analyses, persistence and forecast at the 3-day and 6-day range) upon the original CORIOLIS profiles locations.

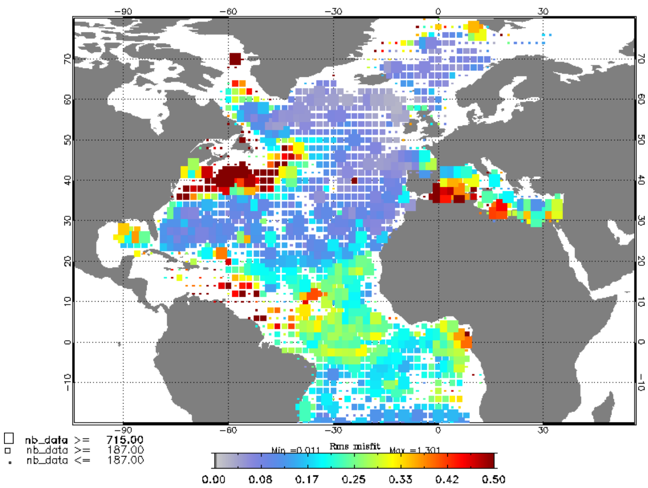

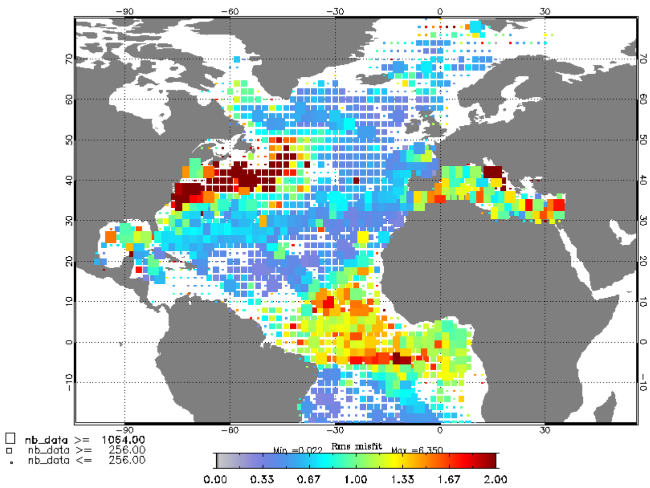

Figure 2: RMS of PSY2V4R1 departures from CORIOLIS observations in the 5-100m layer for salinity (psu, left panel) and temperature (℃, right panel), for the whole 2007-2 010 period (in QuO Va Dis? #3).

They allow assessing the accuracy of the analyses as well as the quality of the forecast. Statistics are performed in layers over geographical regions (ocean basins or smaller), or binned into 2°x2° boxes, as shown in Figure 2. In t his diagnostic the size of the pixel depends on the number of profiles used for the statistic. Through our participation in the MyOcean product quality and cal/val working group, we decided to improve these statistics in the future by performing a weighting by model layer thicknesses (here the only weight is the number of observations). These diagnostics have also been used for the calibration of the monitoring and forecasting systems on several years of hindcast (here 2007-2010).

CLASS4 collocated model equivalents also allow us producing potential temperature *vs.* salinity diagrams in dynamically consistent regions. These graphs offer a different view on the models' representation of water masses and oceanic processes (for instance Mediterranean outflow in the Atlantic in Figure 3).

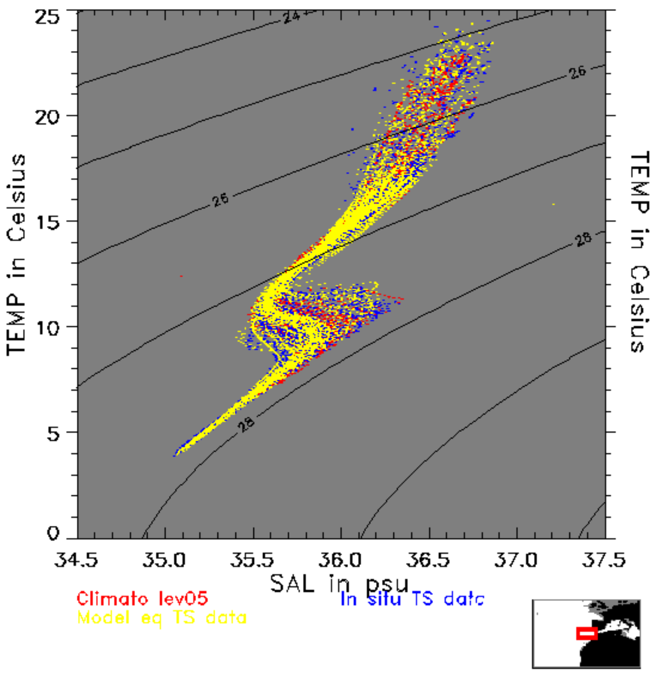

Figure 3: Salinity (psu) versus potential temperature (°c) in October-November-December 2010 (from QuO Va Dis ? #3) in the region of the Gulf of Cadiz. In red values from WOA05 climatology, in blue values from CORIOLIS in situ profiles, in yellow values from PSY2V4R1, all collocated on the CORIOLIS profiles.

Skill scores have also been computed from CLASS4 colocations, as can be seen in Figure 4. The Murphy Skill Score (see for instance Wilks, 2006) is described by Equation 1. This score is close to 0 if the forecast is equivalent to the reference. It is positive and aims towards 1 if the forecast is more accurate than the reference.

$$SS = 1 - \frac{\sum_{k=1}^{n}\left[\frac{1}{M}\sum_{m=1}^{M}\left(Forecast_m - Obs_m\right)^2\right]}{\sum_{k=1}^{n}\left[\frac{1}{M}\sum_{m=1}^{M}\left(Ref_m - Obs_m\right)^2\right]}$$

Equation 1

Here computed in 4°x4° boxes and on the 0-50m layer , the skill score shows that the Mercator Ocean forecast better represents the observed situation (CORIOLIS in situ profiles) than the WOA05 climatology in most regions of the world (Figure 43, upper panel). When the forecast accuracy is compared to the persistence accuracy (accuracy of the last analysis), we can notice that the forecast is more pertinent than the persistence in many regions (in yellow Figure 43, lower panel). Nevertheless noise appears and the benefit of the forecast with respect to the persistence is not as spectacular as with respect to the climatology.

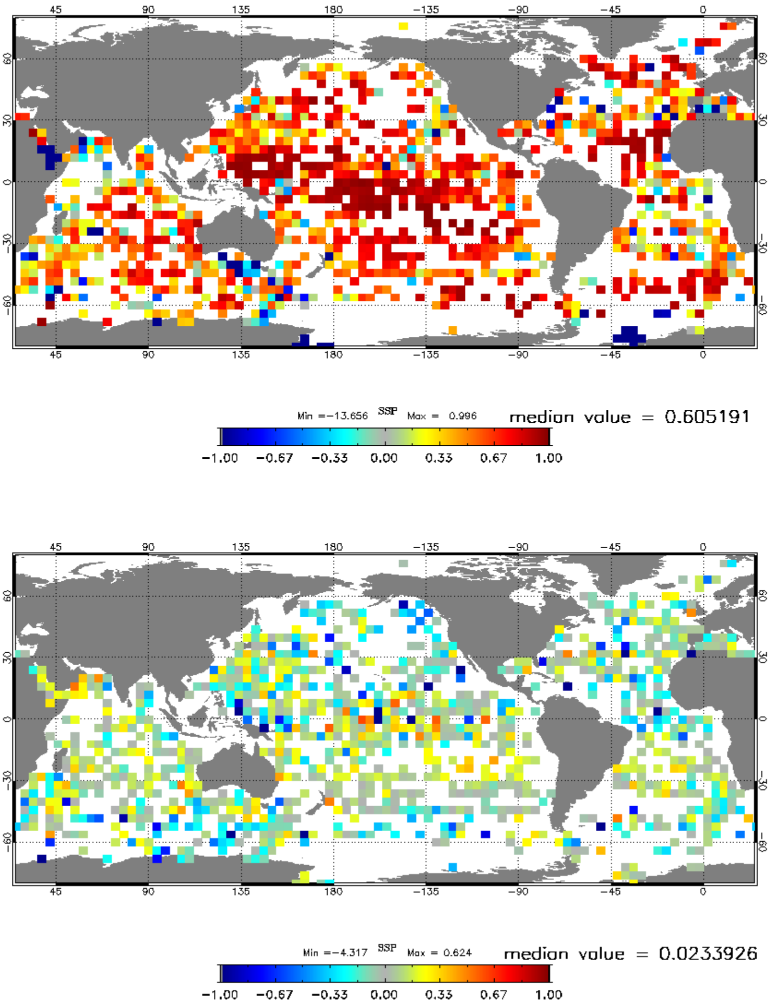

Figure 4: Murphy skill score of the PSY3V3R1 temperature 3-day forecast in the 0-50m layer in January-February-March 2011 (to appear in May in QuO Va Dis? #4) with respect to climatology (upper panel) and persistence (lower panel).

On going collaborations with CORIOLIS

Deep velocities can be estimated from floats displacements during each submerged phase of the ARGO floats cycle (see YoMaHa'07 description by Lebedev et al., 2007). The ANDRO global dataset from Ifremer spans the whole ARGO period (2002-2010) and gives access to thoroughly qualified deep velocities at parking level as well as to surface velocities. A comprehensive version of the atlas should be released by the end of the year 2011. A comparison of these currents observations around 1000m with outputs from the Mercator Ocean monitoring and forecasting systems (especially GLORYS2V1) is in progress in collaboration with Michel Ollitrault from Ifremer.

Also in the context of the GLORYS reanalysis, a feedback loop was initiated to inform CORIOLIS on which observations from the CORA dataset were rejected by the data assimilation process. This feedback of the forecasting centers towards the observation centers is easier to organise in delayed mode. The next step will be to organise it in near real time, which should be done in the following months.

Conclusion

The *QuO Va Dis?* is still under construction but already offers a general view of Mercator Ocean products quality, using CORIOLIS observations as a reference. It can be obtained by contacting qualif@mercator-ocean.fr (suggestions are welcome too) and will be published on Mercator Océan website in the near future.

References

Lebedev Konstantin V., Hiroshi Yoshinari, Nikolai A. Maximenko, and Peter W. Hacker, *YoMaHa'07: Velocity data assessed from trajectories of Argo floats at parking level and at the sea surface*, IPRC Technical Note No.4(2), 2007

Wilks Daniel S., *Statistical Methods in the Atmospheric Sciences*, Academic Press, 2006

Notebook

Articles:

Contact :

Please send us your comments to the following e-mail address: webmaster@mercator-ocean.fr

Next issue: July 2011